

AN ABSTRACT OF THE THESIS OF

William E. Gallahan III for the degree of Master of Science in Geology presented on September 24, 1990.

Title: Experimental Determination of the Temperature and Compositional Dependences of Rare Earth Element, Y, and Sc Partitioning Between High-Ca Clinopyroxene and Natural Mafic to Intermediate Silicate Melts

Abstract approved: _____

Roger L. Nielsen

To understand the differentiation of magmatic systems it is necessary to know the partitioning behavior of the trace elements in evolving mafic magmas. Specifically, understanding the effects of composition and temperature on the partitioning behavior of petrogenetic indicators, such as the rare earth elements, in major fractionating phases is imperative to the development of accurate models for describing mineral-melt equilibria. Historically, models of igneous differentiation have assumed fixed mineral/melt elemental ratios (D's), thus ignoring the effects of changing temperature and composition.

In this experimental study I have investigated the effects of composition and temperature on the partitioning behavior of REE, Y, and Sc between high-Ca clinopyroxene and natural mafic to intermediate silicate systems. Charge-balancing substitution mechanisms for the trivalent trace elements in clinopyroxene were determined by examination of the covariation of major elements in the experimental phases. Using these substitutions, mineral-melt equilibria reactions for trace element clinopyroxene components were defined. The calculated equilibrium constants for these reactions are significantly less dependent on composition, when compared to partition coefficients for the same elements. Regression of these equilibrium constants over the experimental temperature range (1180-1050°C) produced expressions which, when applied to the experimental glasses, reproduce the clinopyroxene trace element contents with a precision of 7-20% (1σ).

These new partitioning expressions were included in a model of igneous differentiation. The results of calculations using this model were compared with results of calculations based upon published elemental mineral/melt distribution

coefficients. The new expressions suggest that REE ratios (e.g. La/Sm) are significantly less sensitive to fractionation involving pyroxene than previously believed. Thus, REE ratios are more likely to be indicative of a mantle derived signature, or alternatively, of the REE signature of a contaminant.

Experimental Determination of the Temperature and Compositional Dependences
of Rare Earth Element, Y, and Sc Partitioning Between High-Ca
Clinopyroxene and Natural Mafic to Intermediate Silicate Melts

by

William E. Gallahan III

A THESIS

submitted to

Oregon State University

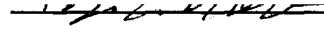
in partial fulfillment of
the requirements for the
degree of

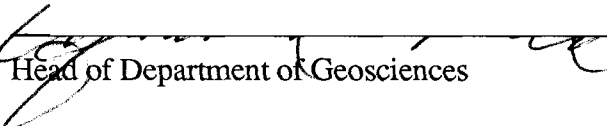
Master of Science

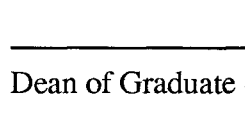


Completed September 24, 1990

Commencement June 1991

APPROVED:


Assistant Professor of Geosciences in charge of major


Head of Department of Geosciences

 Dean of Graduate School  

Date thesis is presented September 24, 1990

Typed by researcher for William E. Gallahan III

ACKNOWLEDGEMENT

The completion of my thesis marks the culmination of a period of intense education and nurturing, directed primarily by my advisor, in one of the more esoteric subdisciplines in geology, thermodynamics. Without his seemingly infinite patience with my questions (many of which have been repeated in the past two years) regarding thermodynamics, this thesis would not have been possible. In addition to the continual tutoring, guidance, and knowledge, he has provided a friendship which is rare between an advisor and a student. To him, Roger Nielsen, I give my greatest thanks.

I wish to extend thanks to my graduate committee members, Cyrus Field, Anita Grunder, and Martin Fisk, for their constructive timely reviews of my thesis drafts. Special recognition goes to the geosciences and oceanography faculty who have provided exceptional instruction in the formal courses I have taken in the past two years. Your instruction has provided me with the background necessary to further my education in a Ph.D. program. The demonstrated concern by each of you, for the educational needs of the students, is a credit to you all.

Discussions with Todd Dunn at the University of New Brunswick, and Gordon McKay at the Johnson Space Center, have provided valuable insight and suggestions which improved this thesis considerably.

Finally, my salary as a research assistant under N.S.F. grant EAR 8720683 provided the necessary financial support which allowed the completion of this thesis in a timely manner. Much thanks is extended to N.S.F. for its continuing support of graduate student research during a time of dwindling financial resources.

TABLE OF CONTENTS

INTRODUCTION	1
THEORY	3
DETERMINATION OF DISTRIBUTION COEFFICIENTS	5
Natural Phenocryst-Matrix Studies	5
Experimental Studies	5
Temperature and Compositional Effects on Distribution Coefficients	7
PYROXENE CRYSTAL CHEMISTRY	10
MELT CONSIDERATIONS	12
INVESTIGATED ELEMENTS	14
STARTING COMPOSITIONS	16
EXPERIMENTAL TECHNIQUES	19
Sample Preparation	19
Experiments	19
ANALYTICAL TECHNIQUES	21
RESULTS	22
Henry's Law Test	22
Equilibration Times	22
Quench Effects and Sector Zoning	24
REE and Y Partitioning	25
Sc Partitioning	30
INTERPRETATION OF RESULTS	32
REE and Y Partitioning	32
Sc Partitioning	39

TEST OF MODEL	43
APPLICATION OF REGRESSIONS	47
CONCLUSIONS	51
REFERENCES	52
APPENDIX	57

LIST OF FIGURES

<u>Figure</u>		<u>Page</u>
1	Experimentally determined distribution coefficients as functions of inverse temperature from previous 1 atmosphere studies of (a) Sm and (b) Sc.	7
2	Compositional ranges of experimental systems in this study. Open squares are starting compositions, filled squares are experimental products. (a) Total alkalis vs SiO ₂ , (b) Al ₂ O ₃ vs SiO ₂ , (c) Al ₂ O ₃ vs FeO*, and (d) MgO vs FeO*. FeO* = All Fe as FeO.	16
3	Experimentally determined distribution coefficients for La as a function of doping level of the charges. La is expressed in cation normalized mole fractions.	22
4	Variation of distribution coefficients as a function of run duration for the systems (a) E-1, (b) GC-68, and (c) ML-190.	23
5	Partitioning behavior calculated from the results of microprobe analyses of experimental charges, expressed as logarithm of distribution coefficients vs inverse temperature for (a) La, (b) Sm, (c) Gd, (d) Ho, (e) Lu, and (f) Y.	25
6	Correlation of (1090-1110°C) REE distribution coefficients with (a) Al content of melt, (b) wollastonite content of clinopyroxene, (c) Ti content of clinopyroxene, and (d) distribution coefficient of Ti.	27
7	REE distribution coefficients vs (a) Ti content of melt, (b) Fe/Mg ratio of clinopyroxene, (c) Fe/Mg ratio of melt, and (d) fO ₂ of the system (filled squares are at QFM, open squares are at 1.2-1.5 log units above QFM). Data from 1090-1110°C experiments only.	29
8	Calculated partitioning behavior of Sc, expressed as logarithm of distribution coefficients vs inverse temperature.	31

<u>Figure</u>	<u>Page</u>
9	31
Covariation of major elements with Sc in clinopyroxenes.	
10	32
Compensated partition coefficients for Sm, calculated by applying two-lattice melt component activity model.	
11	34
Correlation of D_{Ti} with Al content of the melt.	
12	36
Plot of the logarithm of calculated equilibrium constants for mineral-melt equilibria reactions of clinopyroxene components for (a) Sm, (b) La, (c) Gd, (d) Ho, (e) Lu, and (f) Y.	
13	39
Compensated partition coefficients for Sc, calculated by applying two-lattice model component activity model.	
14	41
Relationship of Sc content in the clinopyroxene with the tetrahedral Al, as calculated by equation 25, available to charge balance a $CaScAlSiO_6$ component. Plot of linear regression, equation 26, is shown.	
15	42
Plot of the logarithm of calculated equilibrium constants for mineral-melt equilibria of Sc clinopyroxene component.	
16	43
Test results on internal precision of defined linear regressions (equations 13-18, 28) for (a) La, (b) Sm, (c) Gd, (d) Ho, (e) Lu, (f) Y, and (g) Sc.	
17	45
Results of applying linear regressions to previous experimental results on (a) Sm: filled squares from current study, open squares from McKay et al. (1986), filled diamonds from Mysen and Virgo (1980), and open diamonds from Ray et al. (1983); (b) Lu: filled squares from current study, open square from McKay et al. (1986); and (c) Sc: filled squares from current study, open squares from Lindstrom (1976), filled diamonds from Ray et al. (1983).	

<u>Figure</u>		<u>Page</u>
18	Calculated REE ratios for homogeneous fractional crystallization from 0-75% for Kilauea Iki olivine tholeiite. (a) La/Sm ratios and (b) La/Lu ratios calculated using bulk D's, d* regressions from Nielsen (1988), and K* regressions from current study.	48
19	Comparison of calculated clinopyroxene REE distribution coefficients in olivine tholeiite at three different temperatures with distribution coefficients determined from phenocryst/matrix analyses from calc-alkaline mafic systems. *Data sources of literature D's: Onuma et al. (1968), Schnetzler and Philpotts (1968, 1970).	50

LIST OF TABLES

<u>Table</u>		<u>Page</u>
1	Clinopyroxene site occupancies on the basis of cation radius and valence. Ionic radii taken from Henderson (1986).	11
2	Published 1 atmosphere experimental data for Sc, Y, and REE partitioning between clinopyroxene and silicate liquids.	15
3	Starting compositions.	18
4	Experimental run conditions.	19
5	Comparison of D_{La} calculated from mineral/melt ratios of microprobe analyses and calculated from La $L\alpha$ X-ray intensity ratios.	21

EXPERIMENTAL DETERMINATION OF THE TEMPERATURE AND
COMPOSITIONAL DEPENDENCES OF RARE EARTH ELEMENT, Y, AND Sc
PARTITIONING BETWEEN HIGH-Ca CLINOPYROXENE AND NATURAL
MAFIC TO INTERMEDIATE SILICATE MELTS

INTRODUCTION

One of the primary focuses in igneous petrology is the modeling of the differentiation processes which produce the observed variety of igneous rocks. An understanding of the mineral-melt equilibria of the major and trace components within any system is basic to describing the geochemical effects of these processes. Our understanding of the relative roles of igneous processes has changed through the years, from Bowen's reaction series (Bowen, 1928) to Rayleigh fractionation (Neumann, 1948; Holland and Kulp, 1949; Neumann et al., 1954) to open system processes (O'Hara and Mathews, 1981; DePaolo, 1981; Hildreth et al., 1986; Leeman and Hawkesworth, 1986; Nielsen, 1988,1989; Defant and Nielsen, 1990). However, because elemental partitioning behavior varies as functions of temperature and composition, particularly for the trace elements, we have been limited in the range of compositions and processes which can be quantitatively modeled.

Many attempts to derive expressions that model the effects of igneous processes on the geochemical evolution of magmas have been made (Greenland, 1970; Allegre et al., 1977; Minster et al., 1977; Allegre and Minster, 1978; O'Hara and Mathews, 1981; DePaolo, 1981). Because of the relatively large variations in trace element abundances caused by differentiation, considerable efforts have been directed toward modeling the systematics of these petrogenetic indicators. However, because of a lack of experimental data, the activity-composition relationships for most trace components in natural silicate melts remain undefined. Thus, it has not been possible to calculate expressions describing the temperature and bulk compositional dependences of trace element partitioning behavior for most systems (Irving, 1978; Colson et al., 1987; Nielsen, 1988)

One area with a demonstrated lack of experimental information is the REE activity-composition relations, and the partitioning behavior of these elements between clinopyroxene and natural silicate melts. Consequently, fixed mineral-melt ratios (D 's) for REE are commonly used to model differentiation processes involving

clinopyroxene for a wide range of temperatures and compositions even though the existing experimental data suggests a large temperature dependence on the partitioning behavior of these important petrogenetic indicators (Nielsen, 1988).

This experimental study has investigated the temperature and compositional effects on trace element partitioning behavior between clinopyroxenes and mafic to intermediate composition melts. An experimental data base of coexisting equilibrium clinopyroxene-melt pairs for a wide range of natural compositions (doped with Sc, Y, La, Sm, Gd, Ho, Lu) was produced and the partitioning behavior of the doped elements determined over a range of experimental temperatures (1050-1180°C). Compositional effects on trace element partitioning were reduced by defining melt component activities using a two lattice melt model (Nielsen, 1988) and clinopyroxene component reactions. Regression of the data over the experimental temperatures defined expressions which, when applied to the modeled natural systems, predict trace element partitioning as functions of temperature and composition with a precision of 7-20% (1σ).

THEORY

Most models of igneous differentiation include some variation of fractional crystallization. Inherent to these models is the use of distribution coefficients, or D's, to estimate the mineral-melt equilibria for the elements in the system. These distribution coefficients can be related to the general expression for chemical equilibrium (Eq. 1). At equilibrium, the difference in chemical potential between any two phases in a system (e.g. minerals and melt) can be described as:

$$\Delta\mu_i = 0 = -\ln(a_i^{xtl}/a_i^{liq}) + A/T + B \quad 1$$

where a_i^{xtl} and a_i^{liq} are the activities of component i in the mineral and melt respectively; T is the absolute temperature; and, A and B are regression constants which define the enthalpy and entropy of mixing, respectively.

By rewriting equation 1, the following expression results:

$$\ln(a_i^{xtl}/a_i^{liq}) = A/T + B \quad 2$$

The relationship of distribution coefficients with equation 2 can be derived from several simplifying assumptions and algebraic manipulations. These manipulations are outlined below.

If temperature is assumed constant, then Equation 2 can be reduced to:

$$\ln(a_i^{xtl}/a_i^{liq}) = C \quad 3$$

where C is a constant. Raising the exponent by each side of Equation 3 yields:

$$(a_i^{xtl}/a_i^{liq}) = C' \quad 4$$

where C' is constant.

Using Nernst notation to describe the activities of component i as:

$$a_i = \gamma_i X_i \quad 5$$

where γ_i is the activity coefficient and X_i is the mole fraction of component i , each side of Equation 4 can be multiplied by the inverse of the ratio of activity coefficients. Thus, yielding the expression for the distribution coefficient, D , at a constant temperature:

$$D = X_i^{\text{xtl}} / X_i^{\text{liq}} \quad 6$$

Equation 6 neglects the compositional and temperature effects on component activities and therefore, is not a description of the activities. Rather, it is an empirical description of the distribution of an element between two phases, without compensating for the temperature and composition of the specific system.

Because D 's can be determined without experimental or thermodynamic constraints, analytically derived fixed values for D are commonly used to model the geochemical evolution of igneous suites. In addition, because the temperature, pressure, and compositional effects on trace element activities are ignored in D 's, it has been difficult, without a large experimental data base, to deconvolute the effects of each of these variables in order to accurately describe the activity-composition relationships in natural systems. This has been one of the major goals in experimental petrology and trace element geochemistry (Irving, 1978; Colson et al., 1988; Nielsen, 1985, 1988) and is the theme of this paper.

DETERMINATION OF DISTRIBUTION COEFFICIENTS

Natural Phenocryst-Matrix Studies

Most trace element distribution coefficients in the literature were determined from the analyses of phenocryst-matrix pairs separated from porphyritic rocks. Several assumptions in this technique may introduce errors in the calculation of D's. For example, the phenocrysts are assumed to have been in equilibrium with the melt (matrix). This does not account for the possibility of non-equilibrium phenocrysts or xenocrysts which are optically undetectable in mineral separations. In addition, phenocrysts are assumed to be pure and homogeneous. Problems with accessory phase inclusions resulting in anomalously high D's for incompatible elements have been well documented (Michael, 1988; Sisson, 1989). Finally, temperatures and oxygen fugacities of the magma must be inferred from geothermometry and oxybarometry, with potentially large additive error. As a result of all these factors, reported trace element distribution coefficients may vary by several orders of magnitude for chemically similar systems (Henderson, 1986). Consequently, independently determined temperature and compositional effects on D's have been difficult to define from natural phenocryst-matrix pairs (Lemarchande, 1987).

Experimental Studies

The favored approach for the determination of trace element distribution coefficients has been by direct experimentation (e.g. Drake, 1972; Leeman, 1974; Lindstrom, 1976; Mysen and Virgo, 1980; Ray et al., 1983; Colson et al., 1988, 1989; McKay 1986; McKay et al., 1986). Experimentally determined partitioning behavior has the advantage that the physiochemical variables of a system (temperature, pressure, and composition) can be controlled. Consequently, many sources of error in determining the dependencies of D are eliminated. For example, the crystals are known to originate from the melt, thus eliminating the problem of xenocryst inclusion. In addition, the problem of impure mineral separation is eliminated by *in situ* analyses.

The majority of experimental studies use some method of doping, where the trace elements have been added to the charge (Leeman, 1974; Lindstrom, 1976; Ray et al., 1983; Colson et al., 1989; McKay, 1986; McKay et al., 1986; Dunn, 1987). The doping levels are usually in the wt. % range and are required to facilitate electron microprobe analysis. However, the effects of the high concentration levels on D and

the applicability of the results from these studies to natural systems must be determined.

One technique for assessing the applicability of data from doped experiments to natural systems is by examining the effect of trace element concentration levels on their D's (Henry's Law). Henry's Law behavior is limited to concentration levels where the activity coefficient of the trace elements remain constant, but not necessarily one. Thus, the activity of an element defined by Henry's Law may be expressed:

$$a_i^j = k_i^j X_i^j \quad 7$$

where a_i^j is the activity of element i in phase j ; X_i^j is the mole fraction of element i in phase j ; and, k_i^j is the Henry's Law constant for element i in phase j , where k_i^j is a measure of how much the solution deviates from ideal mixing ($k_i^j = 1$).

The critical question for any application is; over what range of X_i^j is k_i^j constant? If the trace element D's at high X_i are comparable to the D's at low X_i , then k_i^j is constant and the results from the doped experimental charges should be applicable over that range of composition.

Trace element partitioning behavior in doped systems has been shown to be consistent with that at natural concentration levels in many experimental systems (Ray et al., 1983). Watson (1985) in a study of the Henry's Law limits for trace element (Ce, Sm, and Tm) concentrations demonstrated that Henry's Law constants extend into the weight percent range. He showed that experimentally determined trace element partitioning is constant from natural concentration levels to "doped" levels. No evidence of an upper limit to Henry's Law is apparent for most systems; yet, the responsibility remains for the experimentalist to show partitioning behavior independent of the dopant levels in each study.

Many of the experimental studies in the literature have been conducted on synthetic systems designed to be analogues of natural systems. Experimental compositions have ranged from three component (diopside-albite-anorthite) basaltic analogues (Ray et al., 1983) to multicomponent (10) basaltic analogues (McKay et al., 1986). Although ternary systems such as diopside-albite-anorthite have been used to model the major element systematics for evolving mafic systems, they lack components which may cause complex interactions in the melt which affect trace element activities (e.g. Ti and P) (Ellison and Hess, 1990; Nielsen and Gallahan, 1990). In addition,

most synthetic system experiments are conducted at temperatures 100-500 degrees above temperatures appropriate for natural melts. Consequently, conclusions regarding natural system behavior that are based upon the experimental results from simplified synthetic systems are suspect.

Temperature and Compositional Effects on Distribution Coefficients

The temperature dependence of REE and Sc partitioning between clinopyroxene and synthetic systems can be seen from the 1 atmosphere experimental results of Lindstrom (1976), Mysen and Virgo (1980), Ray et al. (1983), and McKay et al. (1986) (Fig. 1a & b). Partition coefficients determined in these investigations increase as a function of decreasing temperature. Yet, there are demonstrated large variations in D at any single temperature. In addition, the single datum reported by McKay et al. (1986) at 1140°C is offset from the linear trend defined by the results of higher temperature experiments. These variations in partitioning behavior can be attributed to the combined effects of composition and temperature on the activities of trace element components, thus preventing the accurate determination of temperature effects alone.

Figure 1 Experimentally determined distribution coefficients as functions of inverse temperature from previous 1 atmosphere studies of (a) Sm and (b) Sc.

(a)

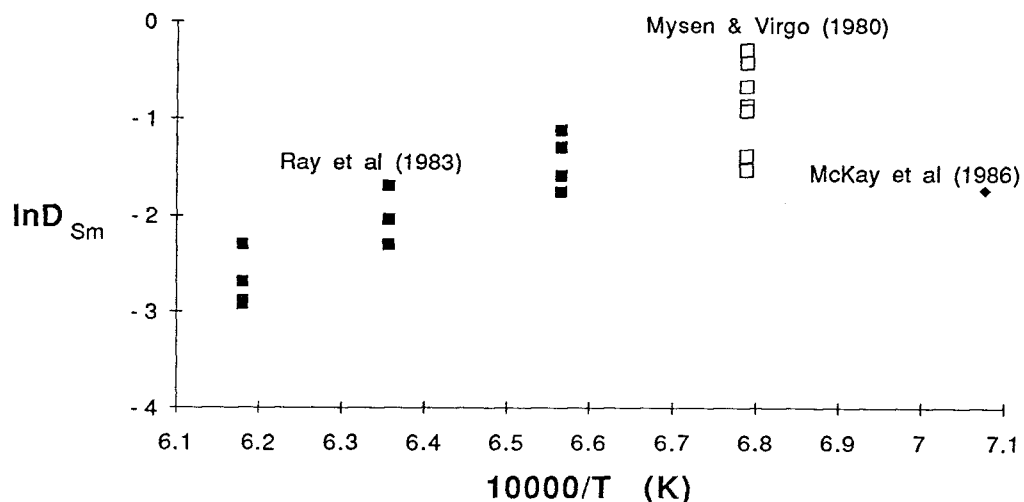
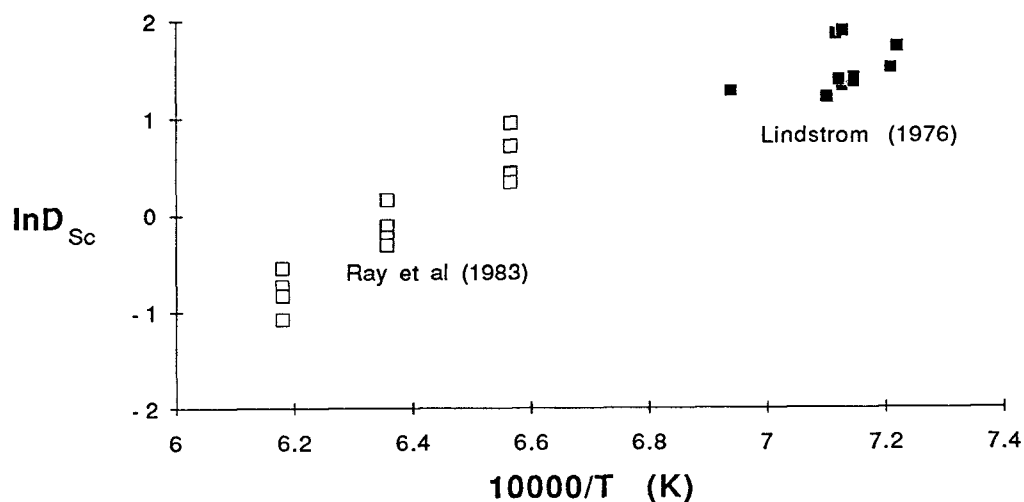


Figure 1 Continued

(b)



The effects of the melt composition on trace element activities in natural silicate systems remain largely undefined. Compositional variations in the melt include changes in the Fe/Mg ratio, which is commonly used to describe the extent of differentiation (McKay et al., 1986). However, because Fe/Mg usually increases as the temperature of a melt decreases it has been difficult to determine the effect of this ratio independent of temperature. Possible effects of Fe/Mg on partitioning behavior can be seen in the results of Leeman (1974) and McKay et al. (1986). In an experimental study of trace element partitioning between olivine and melt, Leeman (1974) positively correlated Fe/Mg with D_{Ni} , D_{Co} , and D_{Mn} . However, this positive correlation between Fe/Mg and D 's can be contrasted with the results of McKay et al. (1986), who experimentally investigated Sm partitioning between clinopyroxene and Fe-rich melt (Shergottite analog). Their results (Fig. 1a) indicated a lower D_{Sm} than that extrapolated from experimental results of Sm partitioning in Fe-free systems (Mysen and Virgo, 1980; Ray et al. 1983). This lower than expected D_{Sm} in the Fe-rich system may be due to the large Fe/Mg ratio, or another variable not defined in the systems. In any case, the extrapolation of D_{Sm} from the experimental results on higher temperature systems to the lower temperature system of McKay et al. (1986) does not accurately describe Sm partitioning behavior in the Fe-rich system.

The effects of crystal chemistry on trace element partitioning remain largely undefined for clinopyroxenes. McKay et al. (1986) reported a variation of REE distribution coefficients with pyroxene wollastonite content (Wo). Their results

indicated an increase in D with increasing Wo in both pigeonites and augites. In addition, a positive correlation of Wo dependence with decreasing atomic number of the REE's was determined through regression analysis. Thus, D_{La} was found to be more dependent on Wo than D_{Lu} . This suggests that the effects of crystal chemistry are potentially important in a comprehensive study of the partitioning of REE in clinopyroxenes.

PYROXENE CRYSTAL CHEMISTRY

An important consideration in the partitioning of trace elements into pyroxenes is crystal chemistry. How a cation "fits" in the crystallographic structure is determined by lattice site coordinations and valences. In the case of pyroxenes, the incorporation of a trivalent element into either M lattice site, usually occupied by a divalent cation, requires a charge balancing coupled substitution with another element. This constrains the number of available mineral-melt reactions as the substitution mechanism.

The general formula for pyroxene may be expressed as $(M2)(M1)T_2O_6$, where M2 is a distorted, 6 to 8 coordinated lattice site; M1 is an octahedral lattice site; and T are two essentially identical, tetrahedral sites. Site preferences of common pyroxene elements are determined by ionic radii and valence states (Table 1). Monovalent cations, primarily Na, occupy the larger, M2 site. Their relatively large ionic radii and need for paired substitution with a charge balancing trivalent cation in the M1, restrict any intersite mixing.

Divalent cations, depending upon ionic radii, may be restricted to the M2 site or may mix between the two M sites. In clinopyroxenes, the Ca cation, radius^{VI}~1.00Å (Henderson, 1986), occupies the M2 site exclusively. Other major and minor divalent cations such as Mg, Fe, and Mn, are distributed among both the M2 and M1 sites. Trivalent and quadrivalent cations primarily occupy the M1 site. Included among these cations are Fe³⁺, Cr³⁺, and Ti⁴⁺. In addition, Al³⁺ occurs in both the M1 and T sites

For most natural clinopyroxenes formed at low pressure, the tetrahedral T sites (2) are occupied exclusively by Si⁴⁺ and Al³⁺. Because of the small size of the T site and its tetrahedral coordination, Si^{IV} (radius~0.26Å) and Al^{IV} (radius~0.39) (Henderson, 1986) are the major ions which fit the site constraints. However, natural ferri-diopside, containing a significant Fe_{Ts} component (CaFe₂SiO₆), does occur within low Na, oxidized systems (Huckenholz, 1969).

A correlation of pyroxene site occupancies by the major elements with ionic radii, as seen in Table 1, can be extended to determine the site occupancies of trace elements. The ionic radii of the REE range from 1.032Å (La^{VI}) to 0.861Å (Lu^{VI}) (Henderson, 1986). Based upon their ionic radii and similar geochemical behavior, it is assumed that all REE occupy the same crystallographic site (M2). In addition, the valence of the REE requires a charge balancing cation, or site vacancy, accompany the REE in a coupled substitution when replacing the divalent cations that normally occupy the M sites. Because monovalent cations do not generally occupy the M1 site, it is

generally assumed that Al^{3+} substituting for Si^{4+} on a T site is the charge balancing cation (Colson et al., 1989).

Table 1 Clinopyroxene site occupancies on the basis of cation radius and valence. Ionic radii taken from Henderson (1986).

<u>M2 CATIONS^{VI-VIII}</u>	<u>M1 CATIONS^{VI}</u>	<u>T CATIONS</u>
Li^{1+} (0.76-0.92A)	Mg^{2+} (0.72A)	Si^{4+} (0.26A)
Na^{1+} (1.02-1.18A)	Fe^{2+} (0.78A)	Al^{3+} (0.39A)
Mg^{2+} (0.72-0.89A)	Mn^{2+} (0.83A)	Fe^{3+} (0.49A)
Fe^{2+} (0.78-0.92A)	Al^{3+} (0.535A)	
Mn^{2+} (0.83-0.96A)	Cr^{3+} (0.615A)	
Ca^{2+} (1.00-1.12A)	Fe^{3+} (0.645A)	
	Ti^{4+} (0.605A)	

MELT CONSIDERATIONS

Adequately defining melt component activities is imperative to any model which attempts to describe mineral-melt equilibria. Several empirical and theoretical models which attempt to model the melt component activities have been formulated (Richardson, 1956; Toop and Samis, 1962; Bottinga and Weill, 1972; Hess, 1977; Ghiorso et al., 1983; Burnham and Nekvasil, 1986; Nielsen, 1988). However, each of these existing models has proven to be compositionally specific and accurate only within a specific range of pressure, temperature and composition. A major problem in developing such models for trace element applications, has been our inadequate knowledge of the thermodynamics of natural silicate melts, particularly the activity of trace melt components. Without a method for calculating the activities of silicate melt components, we can not derive expressions describing mineral-melt equilibria for trace components that are necessary for completely describing silicate melts.

One approach that has been successful for the calculation of major element melt component activities, is to model melts as regular solutions (Ghiorso and Carmichael, 1985; Ghiorso et al., 1983; Keleman and Ghiorso, 1986; Nicholls et al., 1986). This approach is based upon regression of experimental data, combined with standard state information, to derive the interaction parameters for major components of natural melts in the mafic-to-intermediate compositional range. This method has been applied to model the phase equilibria constraints for a variety of igneous processes. However, the model requires standard state information (enthalpy and entropy) for all mineral and melt components. Such information for many trace components within silicate systems does not exist. Thus, regular solution models cannot readily be applied to trace element partitioning.

Another method for describing silicate melts and component activities is based upon the melt structure model of Bottinga and Weill (1972) in which silicate melts are considered to be composed of two quasi-lattices, network-forming and network-modifying. One variation of this model (Nielsen, 1988) defines the network-forming quasi-lattice as a polymerized network of tetrahedrally coordinated Si, and Al complexed with alkali elements. The network-modifying quasi-lattice consists of Al in excess of alkalis, alkaline earth elements, transition elements, and trace elements as free oxides. Mixing of the components within their respective lattices is assumed to be ideal, with no interlattice mixing. With this assumption, the activities of the melt components can be calculated as the mole fraction of the elements within their

respective quasi-lattice. For example, the REE would be assigned to the network-modifying quasi-lattice and their melt activities ($a_{\text{REE}}^{\text{liq}}$) calculated as;

$$a_{\text{REE}}^{\text{liq}} = X_{\text{REE}}^{\text{liq}} / \Sigma \text{NM} \quad 8$$

where $X_{\text{REE}}^{\text{liq}}$ is the mole fraction of the REE in the melt, and ΣNM is the sum of the mole fractions of the melt components assigned to the network-modifying quasi-lattice. Variations of this method have been used successfully to model mineral-melt equilibria for both major and trace melt components in natural systems (Drake, 1976; Nielsen and Drake, 1979; Nielsen and Dungan, 1983; Nielsen, 1985, 1988); and, it is this approach that is used in the present study.

INVESTIGATED ELEMENTS

The elements Sc, Y, La, Sm, Gd, Ho, and Lu were selected for study for the following reasons. (1) They all have a greater affinity for clinopyroxene than for olivine, plagioclase, or the oxide minerals. (2) Except for Sc, they have similar geochemical behavior. (3) The REE are possibly the most commonly applied petrogenetic indicator in igneous petrology. (4) Scandium is a trivalent trace element that is compatible in clinopyroxene; and, it is incompatible in phases where Y and the REE are compatible such as apatite. Thus the partitioning of Sc is dominated by clinopyroxene. (5) Yttrium has an ionic radius similar to HREE (Henderson, 1982) and therefore should partition similarly (Goldschmidt, 1937). (6) REE dopants spanning the entire lanthanide series were required to account for the variation in partitioning behavior that is normally attributed to the decreasing size of the cation with increasing atomic number (lanthanide contraction).

Investigation of the selected trace elements was important for several reasons. (1) Clinopyroxene is a major fractionating phase for a wide range of temperatures and compositions; and, it is the only major phase, other than garnet and amphibole, which accepts these trivalent cations. Consequently, the partitioning behavior of these elements in clinopyroxene controls their bulk partition coefficients for most basaltic magmas. (2) Previous experimental data indicate a large temperature and compositional dependence of clinopyroxene-melt partitioning for Sc, Y, and REE (Ray et al., 1983; Nielsen, 1988). These dependencies need to be defined to allow for accurate phase equilibria calculations and petrogenetic modeling of common igneous systems. (3) Little of the available data on Sc, Y, and REE partitioning in clinopyroxenes (Table 2) are at temperatures appropriate for differentiation in shallow crustal mafic magma chambers (1050-1200°C).

Table 2 Published 1 atmosphere experimental data for Sc, Y, and REE partitioning between clinopyroxene and silicate liquids.

Ref	Elem	(D)	Mineral	Melt	T(°C)
(1)	Sc	2.2	Augite	Alk basalt	1110-1170
(2)	Sm	0.5	Augite	Ab-An-Fo	1200
(3)	Sc	1.8	Augite	Di-Ab-An	1250-1350
	Sm	0.2			
(4)	Sm	0.17	Augite	Shergottite	1140
	Gd	0.20			
	Lu	0.30			
(5)	Sm	0.022	Pigeonite	Basalt (Lunar)	1200-1345

- (1) Lindstrom (1976)
(2) Mysen and Virgo (1980)
(3) Ray et al. (1983)
(4) McKay et al. (1986)
(5) McKay (1977)

STARTING COMPOSITIONS

To define trace element partitioning behavior between clinopyroxene and evolved natural igneous systems, starting compositions which represent a range of commonly occurring mafic to intermediate composition igneous rocks were selected (Table 3). These natural systems ranged from alkali to tholeiitic basalts, ferrobasalt, and basaltic andesites (Fig. 2a-d). By using these compositions, the relevance of results to natural systems was enhanced. The experimental compositions were chosen on the basis of several criteria, (1) the compositions have clinopyroxene near their liquid, (2) temperatures for equilibrium clinopyroxenes with crystallinity less than 50% span a range of approximately 100°C, which is sufficient for defining the temperature dependence of partitioning, (3) they represent magmas generated in a variety of tectonic settings, including mid-ocean ridges, ocean islands, and arcs, and (4) the calculated liquidus temperatures for clinopyroxene are those normally associated with shallow crustal mafic systems.

Figure 2 Compositional ranges of experimental systems in this study. Open squares are starting compositions, filled squares are experimental products. (a) Total alkalis vs SiO_2 , (b) Al_2O_3 vs SiO_2 , (c) Al_2O_3 vs FeO^* , and (d) MgO vs FeO^* . FeO^* = All Fe as FeO.

(a)

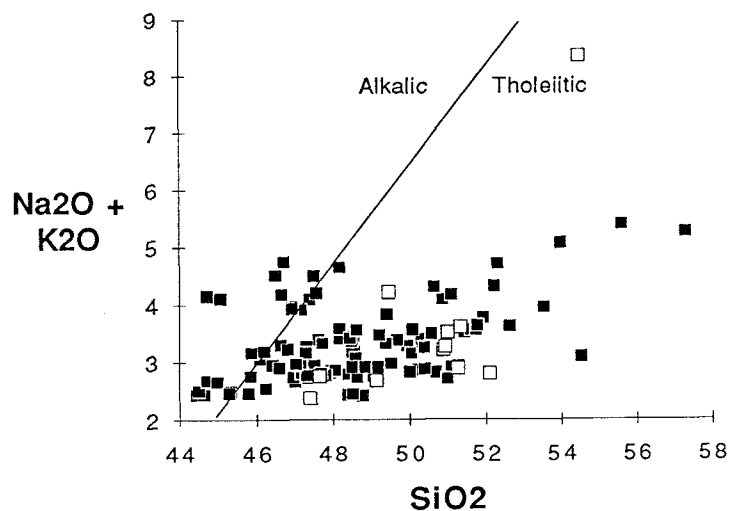
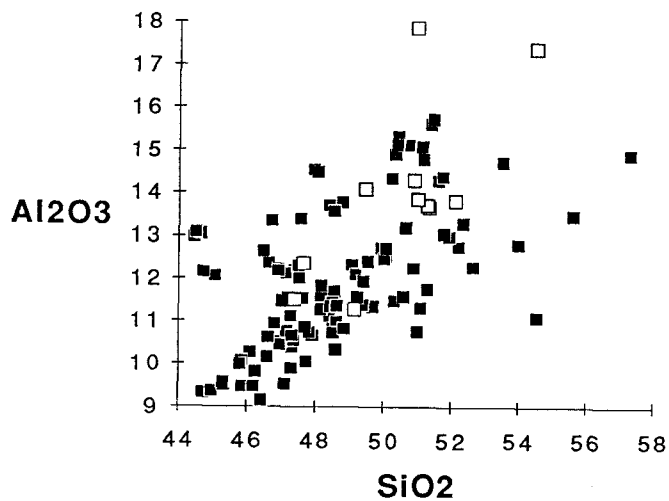
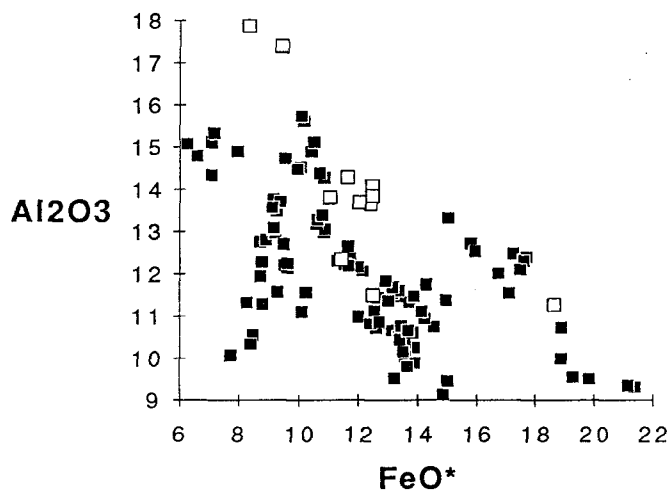


Figure 2 Continued

(b)



(c)



(d)

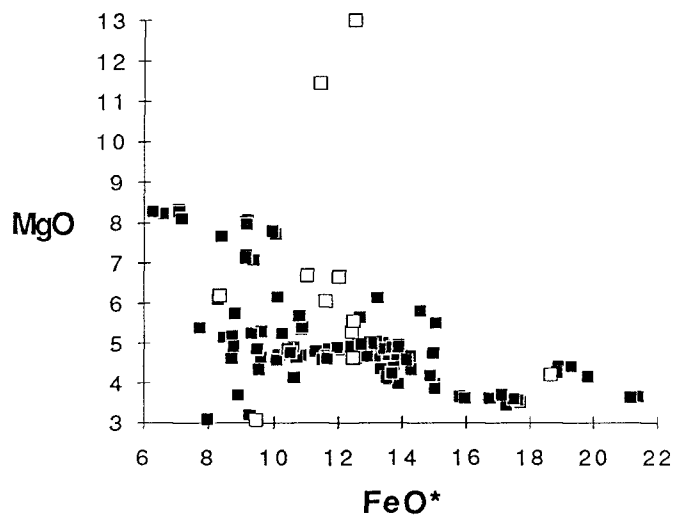


Table 3: Starting compositions.

	H87-3	H87-1	43152	3/83	KL77	E-1	GC-68	ML-190	ML-176	TLW67	2MH005
SiO ₂	47.66	54.50	49.15	50.90	51.34	47.4	49.46	51.29	52.11	51.00	50.95
TiO ₂	2.42	1.74	3.76	3.01	3.69	2.2	4.28	2.08	2.09	3.49	1.38
Al ₂ O ₃	12.35	17.40	11.27	14.29	13.65	11.5	14.09	13.69	13.81	13.85	17.87
Fe ₂ O ₃	1.38	9.45	-----	1.54	1.86	3.7	-----	12.03	-----	2.26	-----
FeO	10.04	-----	18.66	10.08	10.55	8.8	12.47	-----	11.03	10.21	8.34
MnO	0.17	0.25	-----	0.17	0.18	0.18	0.22	0.19	0.18	0.18	0.21
MgO	11.44	3.07	4.21	6.04	5.28	13.0	4.62	6.65	6.68	5.54	6.18
CaO	11.51	4.77	9.33	10.34	9.27	10.4	9.63	10.49	10.63	9.53	11.29
Na ₂ O	2.18	6.00	2.48	2.59	2.82	2.0	3.03	2.51	2.40	2.74	2.32
K ₂ O	0.57	2.35	0.19	0.61	0.79	0.37	1.18	0.38	0.40	0.77	0.95
P ₂ O ₅	0.29	1.22	0.31	0.32	0.40	0.29	1.02	0.23	0.26	0.40	0.51
Reference	3	9	1	4	2	5	6	7	10	8	11

1. Galapagos ferrobalt-Melson (personal communication)
2. Kilauea tholeiite-Moore et al. (1980)
3. Mauna Kea ankaramite-Porter et al. (1987)
4. Kilauea tholeiite-Neal et al. (1988)
5. Uwekahuna Bluff picrite-Casadevall and Dzurisin (1987)
6. Mauna Loa tholeiite-electron microprobe analysis of fused glass beads
7. Mauna Loa tholeiite-Rhodes (1988)
8. Kilauea tholeiite-Wright and Fiske (1971)
9. Kohala hawaiite-Porter et al. (1987)
10. Mauna Loa tholeiite-Rhodes (1988)
11. Mount Hope, AZ A.O.B.-electron microprobe analysis of fused glass beads

EXPERIMENTAL TECHNIQUES

Sample Preparation

The starting compositions were powdered and doped with Sc, Y, and the REE as oxide powders in two batches at 0.5 and 2.0 wt%. Mixtures were ground as acetone slurries, using an alumina mortar and pestle, then fused in graphite crucibles. Two separate groupings of trace elements, one with Sc, Y, and La, and the other with Sm, Gd, and Ho or Lu, were prepared to avoid overlapping X-ray lines (e.g. La and Sm L-lines).

Experiments

Charges of the doped glasses were suspended in a 1 atmosphere Deltech vertical quench, gas mixing furnace. Thin (0.003"-0.005") Pt wire loops were used to reduce Fe loss. Experimental charges were raised above their liquidus for 2-4 hours to assure melt homogeneity. They were then cooled to run temperatures at a rate greater than 500°/hour, held for 1-14 days, and water quenched. Temperatures were measured using a Pt-Pt₉₀Rh₁₀ thermocouple calibrated against the melting point of gold. Oxygen fugacities were monitored with an oxygen electrolyte cell (Williams and Mullins, 1981) calibrated at the iron-wustite buffer. Mixtures of H₂ and CO₂ buffered the oxygen fugacities at the QFM buffer. A list of run conditions for individual charges is shown in Table 4.

Table 4 Experimental run conditions.

System	Charge	Dopants	Dopant Level (wt% oxides)	T (C)	Duration (Hrs)	-log fO ₂
H87-3	0.1	La,Sc	0.1	1180	97	8.71
H87-3	0.5	La,Sc	0.5	1180	97	8.71
H87-3	1.0	La,Sc	1.0	1180	97	8.71
H87-3	0.1	La,Sc	0.1	1150	66	9.09
H87-3	0.5	La,Sc	0.5	1150	70	9.09
H87-3	1.0	La,Sc	1.0	1150	70	9.09
43152	0.1	La,Sc	0.1	1070	68	10.16
43152	1.0	La,Sc	1.0	1070	68	10.16
43152	1d	La,Y,Sc	0.5	1100	68	9.75
43152	4a	La,Y,Sc	2.0	1080	78	10.02
43152	5a	La,Y,Sc	2.0	1071	60	10.15
3/83k	1d	La,Y,Sc	0.5	1100	74	9.75

Table 4 Continued

System	Charge	Dopants	Dopant Level (wt% oxides)	T (C)	Duration (Hrs)	-log fO ₂
KL77	4 a	La,Y,Sc	2.0	1110	50	9.61
KL77	1d	La,Y,Sc	0.5	1100	74	9.75
KL77	2 a	La,Y,Sc	2.0	1090	71	9.88
KL77	3 a	La,Y,Sc	2.0	1087	56	9.93
E-1	a344	La,Y,Sc	2.0	1100	344	9.75
E-1	6 a	La,Y,Sc	2.0	1100	62	9.75
2MH005	2 a	La,Y,Sc	2.0	1120	62	9.48
2MH005	2d	La,Y,Sc	0.5	1100	66	9.75
2MH005	3d	La,Y,Sc	0.5	1100	138	9.75
H87-1	3 a	La,Y,Sc	2.0	1100	62	9.75
GC-68	a192	La,Y,Sc	2.0	1100	192	9.75
GC-68	a72	La,Y,Sc	2.0	1100	72	9.75
GC-68	a344	La,Y,Sc	2.0	1100	344	9.75
GC-68	1d	La,Y,Sc	0.5	1100	95	9.75
ML-190	a192	La,Y,Sc	2.0	1100	192	9.75
ML-190	a72	La,Y,Sc	2.0	1100	72	9.75
ML-190	1d	La,Y,Sc	0.5	1100	96	9.75
ML-176	1d	La,Y,Sc	0.5	1100	51	9.75
TLW67	4 a	La,Y,Sc	2.0	1090	72	9.88
TLW67	6 a	La,Y,Sc	2.0	1100	72	9.75
43152	3 a	La,Y,Sc	2.0	1090	72	9.88
ML-190	a	La,Y,Sc	2.0	1100	118	8.55
E-1	a	La,Y,Sc	2.0	1100	77	8.25
43152	1e	Sm,Gd,Lu	0.5	1100	90	9.75
H87-3	2 b	Sm,Gd,Lu	2.0	1134	120	9.29
3/83k	1e	Sm,Gd,Lu	0.5	1100	144	9.75
KL77	1e	Sm,Gd,Lu	0.5	1100	144	9.75
KL77	5 b	Sm,Gd,Lu	2.0	1090	71	9.88
KL77	1 b	Sm,Gd,Lu	2.0	1106	48	9.66
KL77	3 b	Sm,Gd,Lu	2.0	1085	72	9.95
KL77	4 b	Sm,Gd,Lu	2.0	1076	80	10.08
GC-68	2 e	Sm,Gd,Ho	0.5	1080	96	10.02
ML-190	6 b	Sm,Gd,Ho	2.0	1110	49	9.61
ML-190	1 b	Sm,Gd,Ho	2.0	1101	48	9.73
ML-190	2 b	Sm,Gd,Ho	2.0	1085	72	9.95
ML-176	3 b	Sm,Gd,Ho	2.0	1090	120	9.88
TLW67	1 e	Sm,Gd,Lu	0.5	1100	48	9.75
TLW67	3 e	Sm,Gd,Lu	0.5	1120	359	9.48
2MH005	3 e	Sm,Gd,Lu	0.5	1120	359	9.48
E-1	5 b	Sm,Gd,Ho	2.0	1133	69	9.31
E-1	b	Sm,Gd,Ho	2.0	1100	77	8.25
ML-190	b	Sm,Gd,Ho	2.0	1100	118	8.55
H87-3	3 b	Sm,Gd,Ho	2.0	1140	92	9.22
H87-3	Ho1	Ho	2.0	1165	73	8.90
H87-3	Ho2	Ho	2.0	1133	69	9.31
43152	Ho1	Ho	2.0	1050	67	10.45

ANALYTICAL TECHNIQUES

Analyses for major, minor, and trace elements were accomplished with a Cameca SX-50 electron microprobe. X-ray intensities were measured at 15 kV accelerating potential and 20nA beam current. A partially defocused beam, $\sim 5\mu\text{m}$ diameter, was used to minimize Na diffusion in glass analyses. Counting times (on-peak) were: 10 seconds for major and minor elements, 50 seconds for Sc, and 100 seconds for Y and REE. Background counts were taken above and below the peak for 1/2 the on-peak counting time (e.g. 25 seconds for Sc). Correction of X-ray intensities for deadtime, background, and matrix effects was made using the Cameca PAP routine. Most analyses for mineral-melt pairs were averaged from line traverses containing two to five analyzed points in each phase.

Because of the low La concentrations resulting from its relative incompatibility in clinopyroxenes, a second method was applied for low doped (0.1 & 0.5 wt.%) charges to calculate $D_{\text{La}}^{\text{cpx}}$ and determine the accuracy of the quantitative microprobe analyses. A variation of the technique of McKay (1986) was used at the same beam conditions. Intensities were measured at the peak wavelength for counting times of 1000-2000 seconds then at background offsets on each side of the peak. Net intensities ($I_{\text{peak}} - I_{\text{bgd}}$) in total counts were calculated for clinopyroxene and glass. The ratio of the intensities, $I_{\text{net}}^{\text{cpx}}/I_{\text{net}}^{\text{glass}}$, was compared with $D_{\text{La}}^{\text{cpx}}$, as calculated from full microprobe analyses. As can be seen in table 5, the results were comparable. The full microprobe analyses were used in interpreting the results.

Table 5 Comparison of D_{La} calculated from mineral/melt ratios of microprobe analyses and calculated from La $L\alpha$ X-ray intensity ratios.

CHARGE	T (°C)	$D_{\text{La}} (X_{\text{La}}^{\text{cpx}}/X_{\text{La}}^{\text{glass}})$	$D_{\text{La}} (I_{\text{net}}^{\text{cpx}}/I_{\text{net}}^{\text{glass}})$
H87-3 (0.1% La)	1180	0.081	0.100
H87-3 (0.5% La)	1150	0.086-0.113	0.099

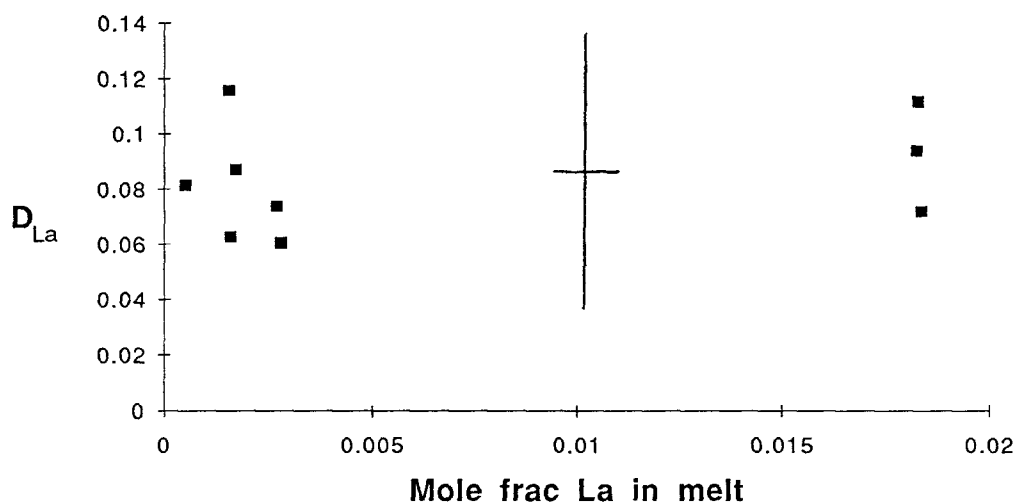
K_2O was included in the analytical routine for clinopyroxene. Because of potassium's incompatibility in pyroxene, it was used as an indicator of glass inclusions. Clinopyroxene analyses containing $\text{K}_2\text{O} > 0.015$ mole % were excluded from the data set. A complete list of microprobe analyses is included in the appendix.

RESULTS

Henry's Law Test

To evaluate the dependence of partition coefficients on elemental concentrations (possible Henry's Law violation), a series of experiments on a single system (H87-3) were conducted at various doping levels at 1180°C. The results (Fig. 3) indicated consistent partitioning behavior over the concentration range of 0.1-2.0 mole % REE in the melt. In addition, the calculated D's are comparable with published data for natural concentrations in similar systems, e.g. Johnson (1989). From these results, it can be inferred that the experiments were conducted within the Henry's Law limits and applicable to systems at natural concentrations.

Figure 3 Experimentally determined distribution coefficients for La as a function of doping level of the charges. La is expressed in cation normalized mole fractions.

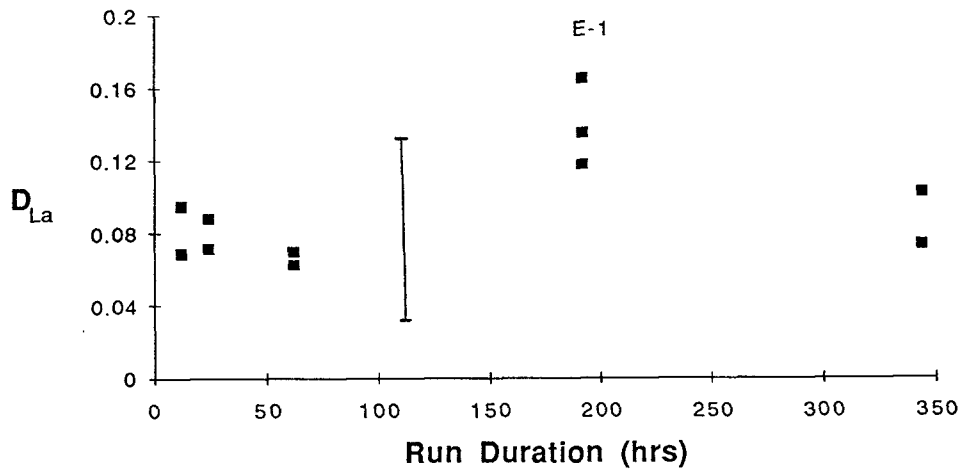


Equilibration Times

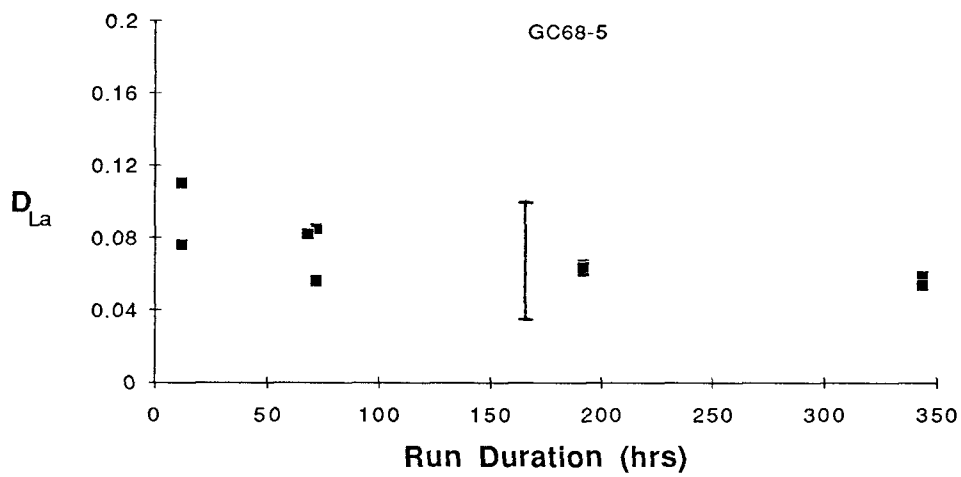
Equilibration times were determined in experiments ranging from 12 to 344 hours at 1100°C with three different starting compositions. Plots of D vs run duration for these experiments (Fig. 4) indicate that consistent partitioning behavior was achieved in ~48 hours. Thus, short duration experiments (48 hrs and less) were excluded from data analysis. Charges with crystallinity $\geq 60\%$, and/or disequilibrium textures, such as resorption and anhedral crystal morphologies, were excluded from data analysis.

Figure 4 Variation of distribution coefficients as a function of run duration for the systems (a) E-1, (b) GC-68, and (c) ML-190.

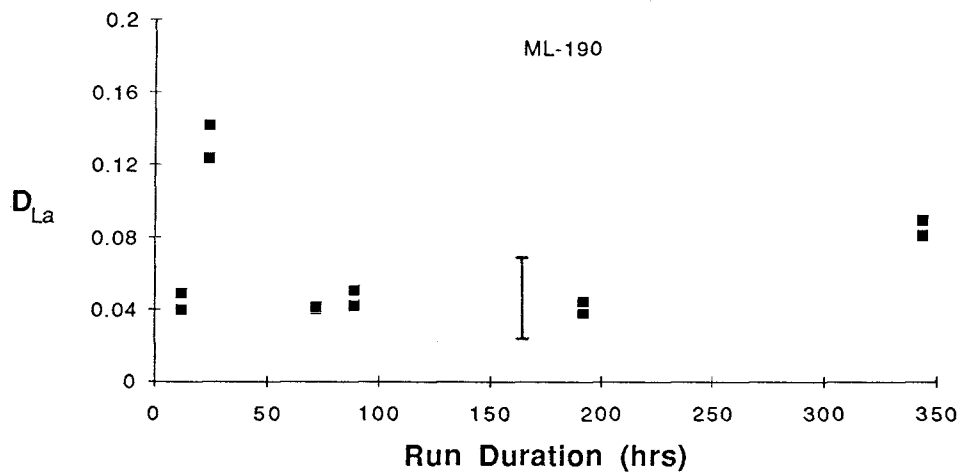
(a)



(b)



(c)

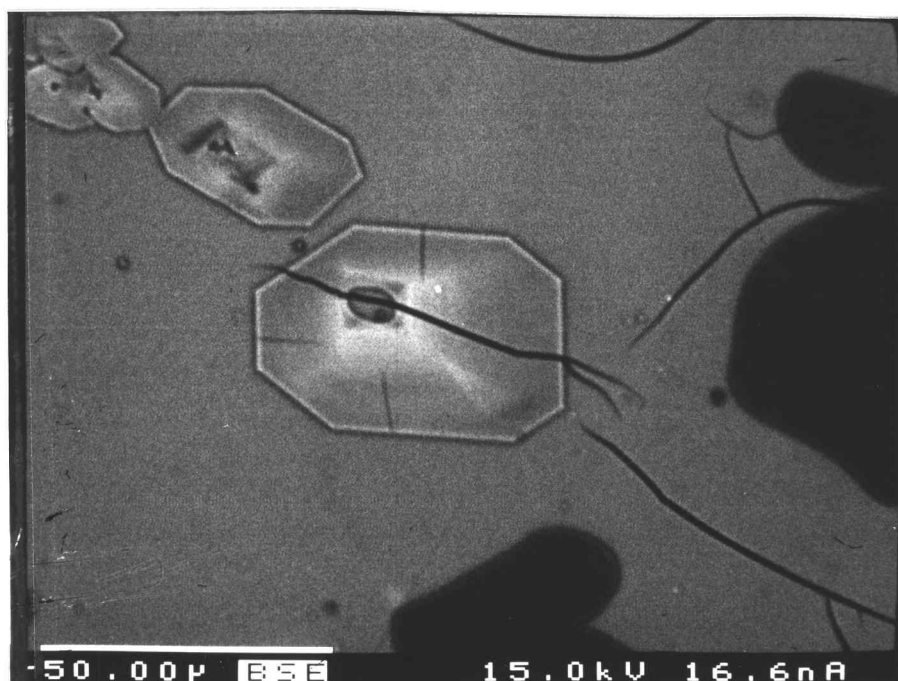


Quench Effects and Sector Zoning

Minor quench growth of olivine was detected optically in approximately 20% of the run products. To avoid the concentration gradients associated with quench olivines (Kring and McKay, 1984), analyses were restricted to clinopyroxenes and glasses at least $30\mu\text{m}$ from these crystals. Also, a SEM backscattered electron image of an experimental charge (Photo 1) revealed a quench rim, $\sim 3\mu\text{m}$ wide, with high Z elements enriched in clinopyroxene and depleted in the surrounding glass. As a result, microprobe analyses were not taken within $10\mu\text{m}$ of clinopyroxene-glass boundaries. It was assumed that the formation of these localized gradients did not effect the overall glass compositions.

Sector zoning was found in several of the experimental pyroxenes (Photo 1). The compositional differences between sectors was most evident in the Ti and Al contents, which varied by as much as 50%. Analysis of REE in these same pyroxenes demonstrated less than 20% increases in the Ti-rich sectors.

Photo 1 SEM back-scattered electron image of an experimental charge revealing quench rim and sector zoning in clinopyroxene (light-colored polygonal phase). Light-colored area surrounding clinopyroxene is glass. Dark phase is olivine.



REE and Y Partitioning

Using the relationship for chemical equilibrium (Eq. 2 & 6), the results of microprobe analyses can be expressed as the logarithm of D as a function of inverse temperature. The results of using D to estimate partitioning behavior can be seen in figures 5a-f. Two characteristics of figures 5a-f can be noted. There are large scatter in D 's at any single temperature; and, the scatter in D 's for each element obscure any obvious temperature effects, with the possible exception of the Lu data.

Figure 5 Partitioning behavior calculated from the results of microprobe analyses of experimental charges, expressed as logarithm of distribution coefficients vs inverse temperature for (a) La, (b) Sm, (c) Gd, (d) Ho, (e) Lu, and (f) Y.

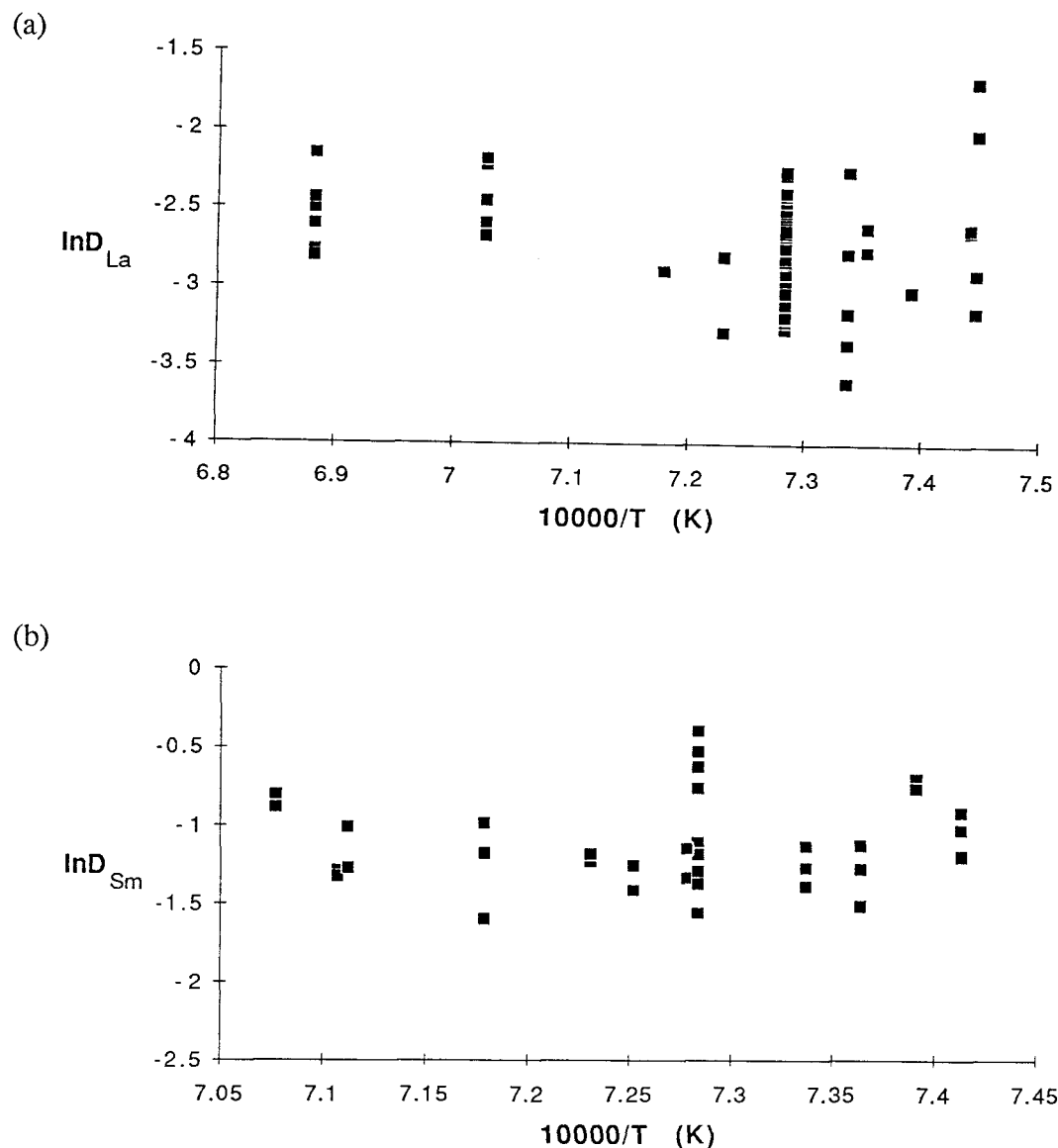


Figure 5 Continued

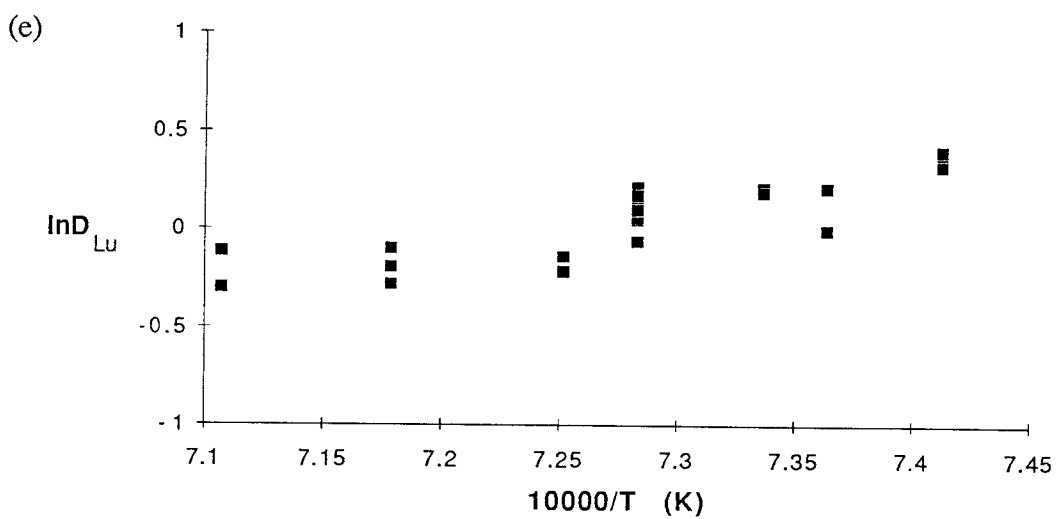
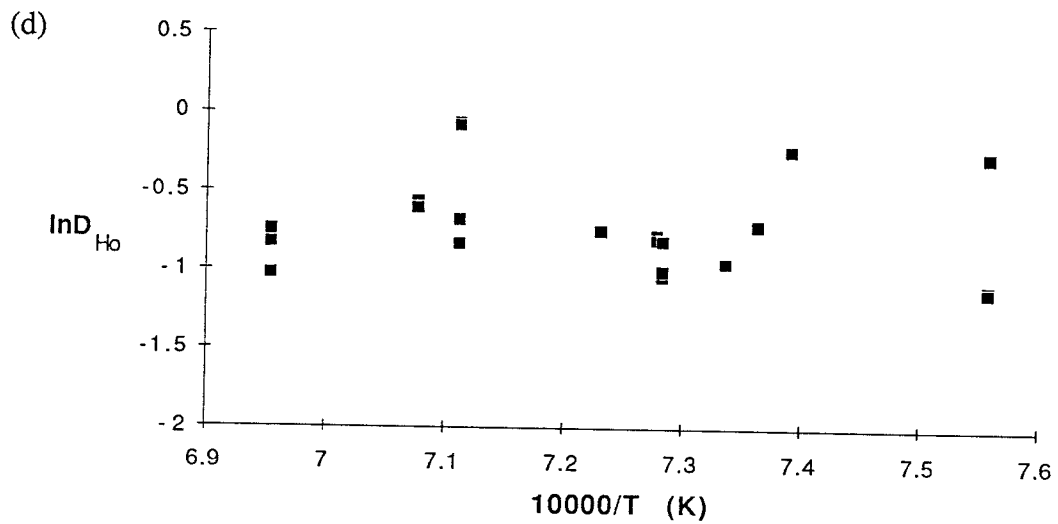
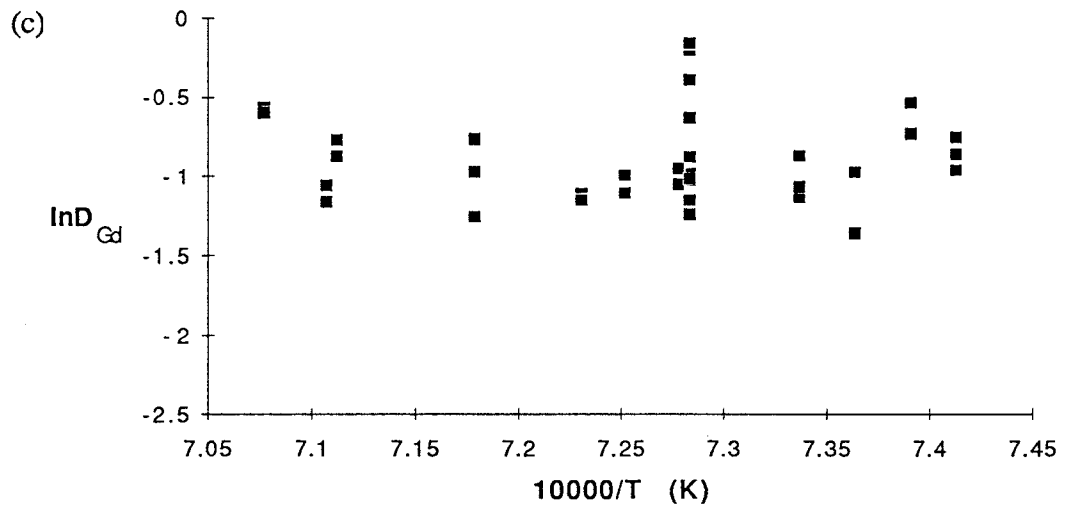
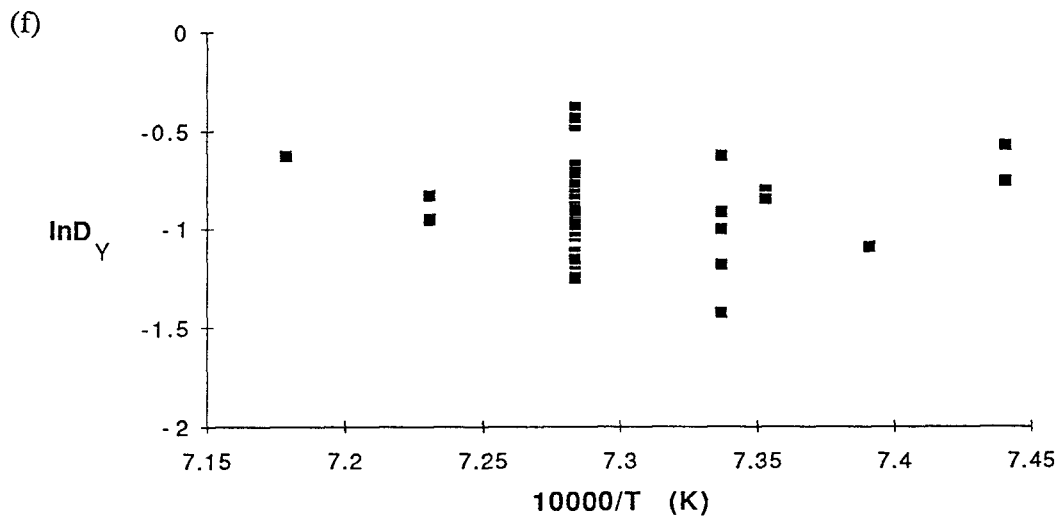


Figure 5 Continued



Factor analysis of experimental data at similar temperatures (1090-1110°C) indicates several relationships with elemental partitioning behavior. First, D_{REE} positively correlate with the mole fraction of Al in the melt (Fig. 6a). Second, D_{REE} positively correlate with Wo in the clinopyroxene (Fig. 6b). Third, D_{REE} positively correlate with the mole fraction of Ti in the clinopyroxene (Fig. 6c). Finally, there is a positive correlation between D_{REE} and D_{Ti} (Fig. 6d).

Figure 6 Correlation of (1090-1110°C) REE distribution coefficients with (a) Al content of melt, (b) wollastonite content of clinopyroxene, (c) Ti content of clinopyroxene, and (d) distribution coefficient of Ti.

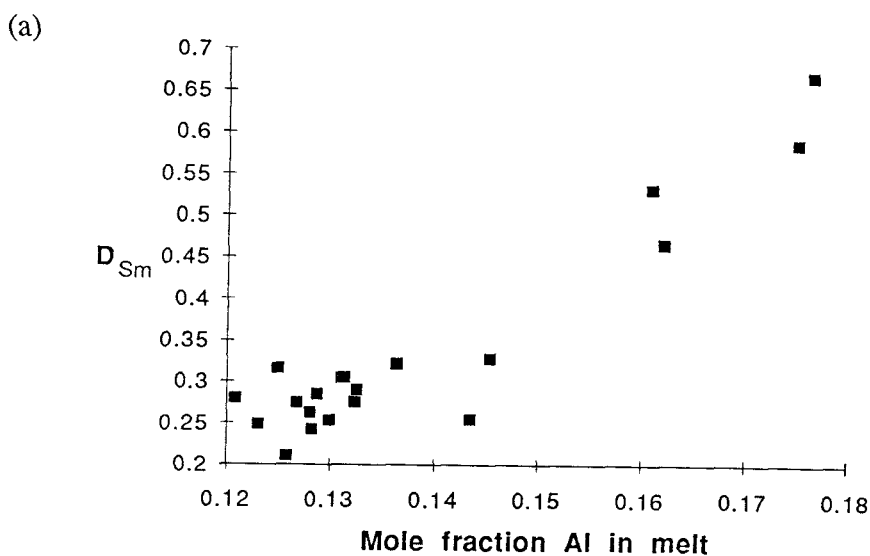
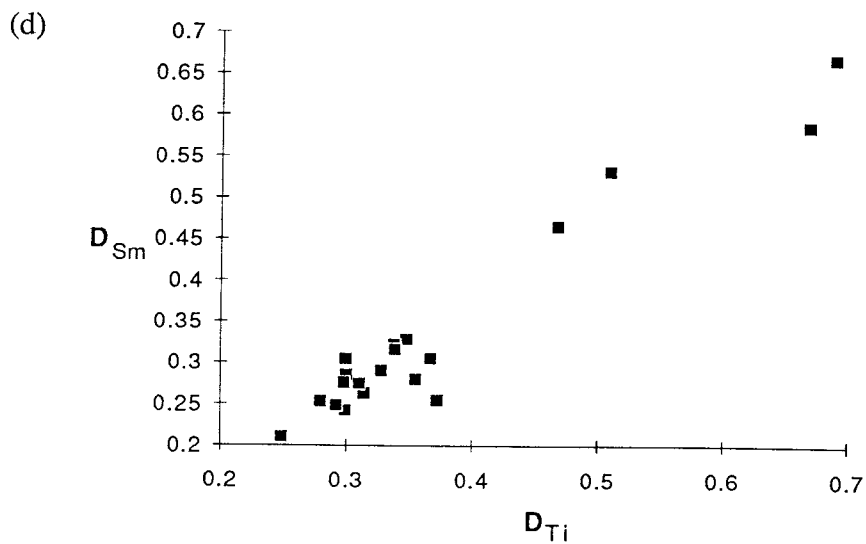
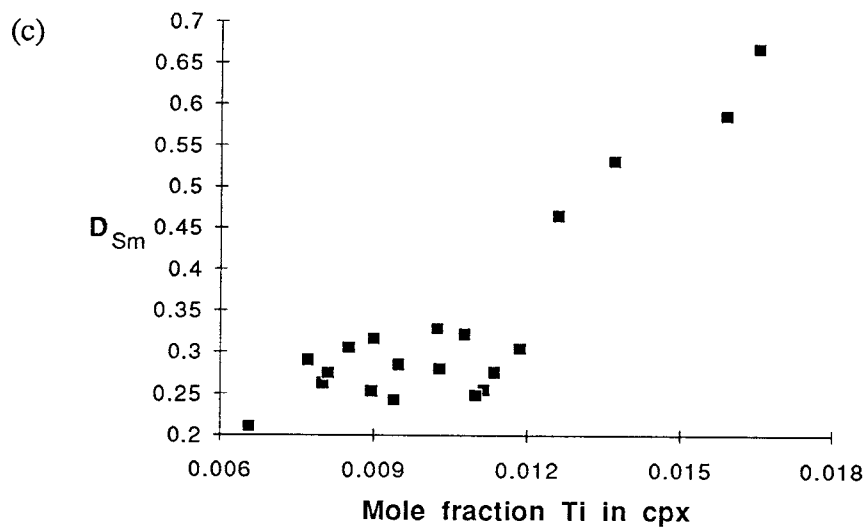
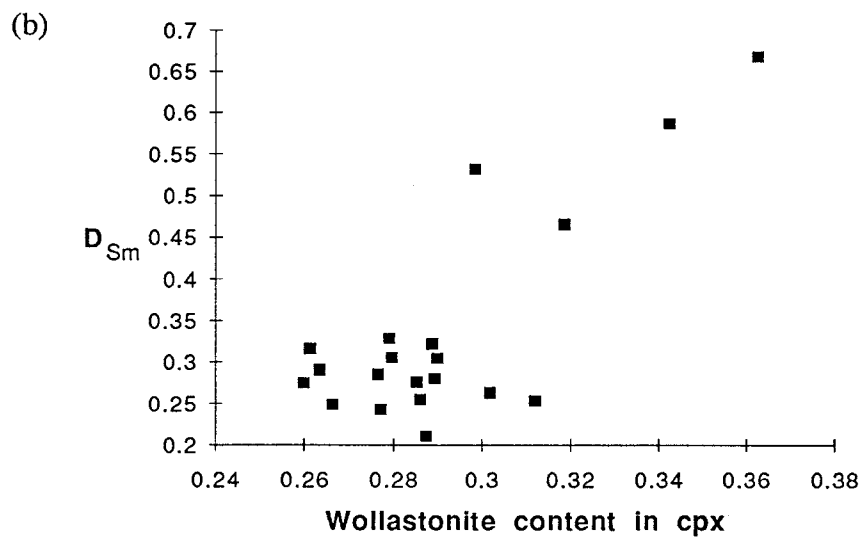


Figure 6 Continued



Additional results from the factor analysis indicated that, (1) partitioning behavior of REE is unrelated to the Ti content of the melt (Fig. 7a), (2) there is no relationship between D_{REE} and the Fe/Mg of the clinopyroxene (Fig. 7b), or the Fe/Mg of the melt (Fig. 7c), and (3) the effect of f_{O_2} on partitioning behavior is minimal (Fig. 7d).

Figure 7 REE distribution coefficients vs (a) Ti content of melt, (b) Fe/Mg ratio of clinopyroxene, (c) Fe/Mg ratio of melt, and (d) f_{O_2} of the system (filled squares are at QFM, open squares are at 1.2-1.5 log units above QFM). Data from 1090-1110°C experiments only.

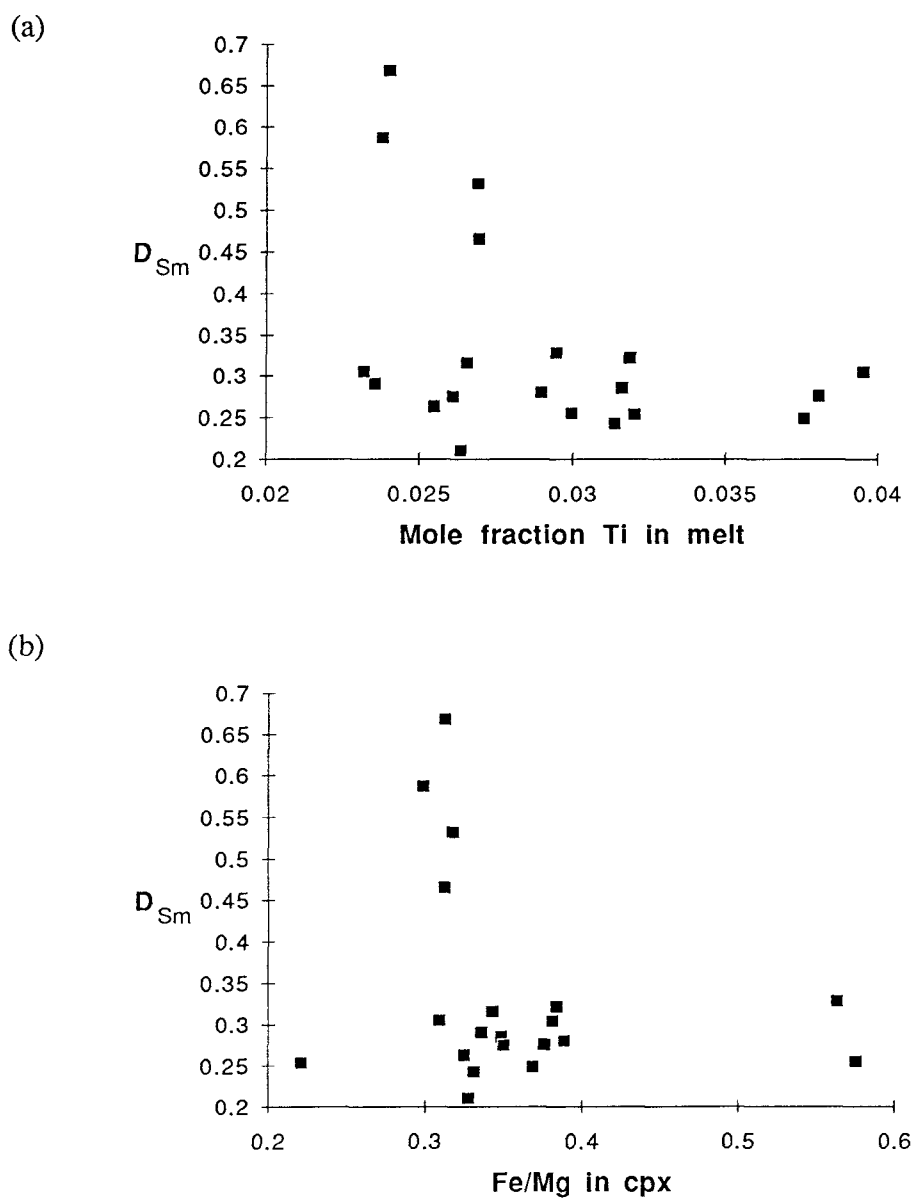
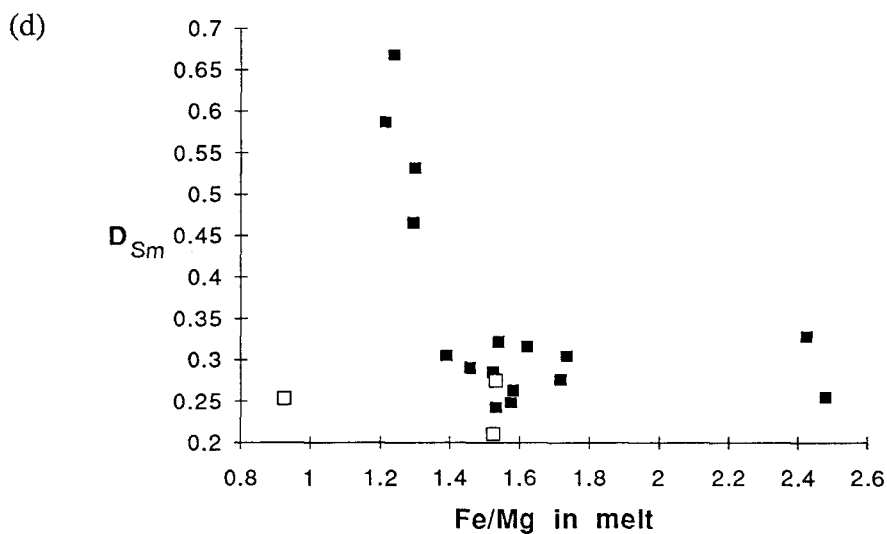
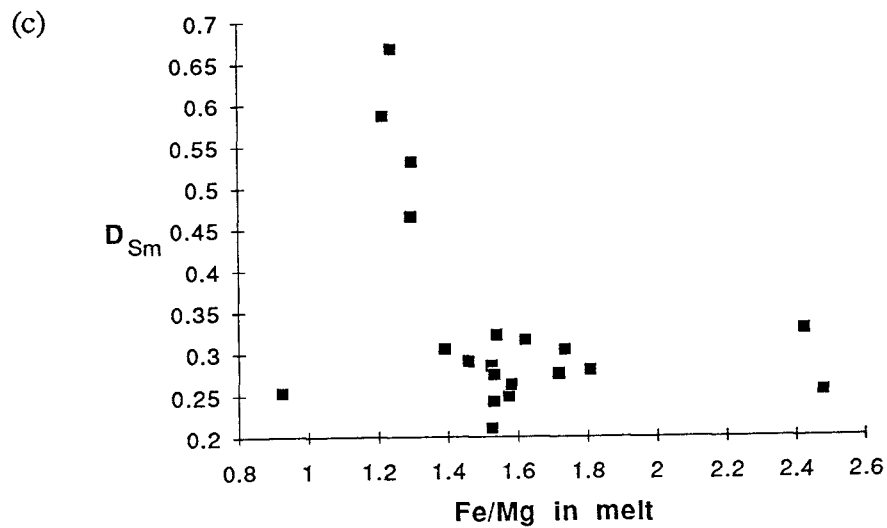


Figure 7 Continued



Sc Partitioning

The analytical results for Sc partitioning can be expressed as a function of reciprocal temperature (Fig. 8). As with the REE data, there are large scatter in D's at each temperature. Any temperature dependence of the D's is obscured, by the observed scatter. Covariation of major element constituents in the clinopyroxenes indicates an increase in Al, and a lesser extent Na, with increasing Sc content. A corresponding decrease in Mg content is indicated (Fig. 9).

Figure 8 Calculated partitioning behavior of Sc, expressed as logarithm of distribution coefficients vs inverse temperature.

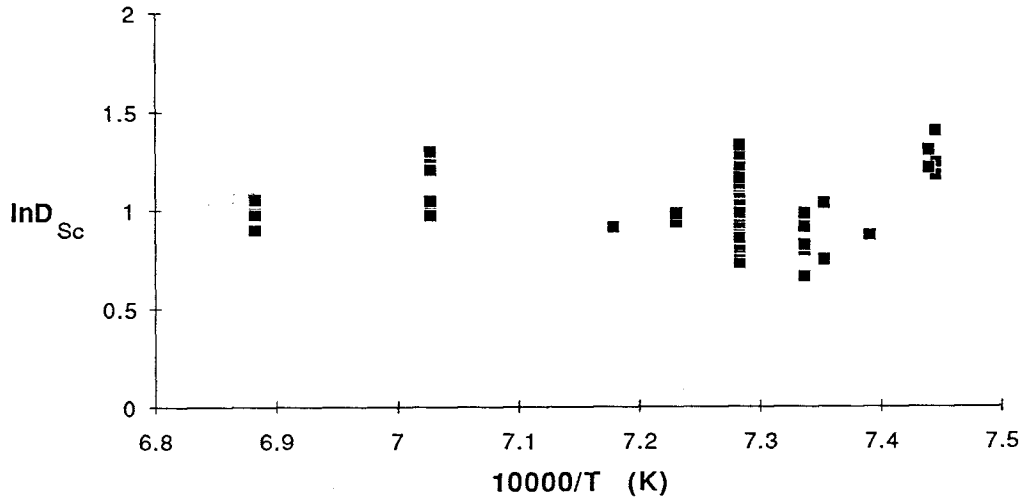
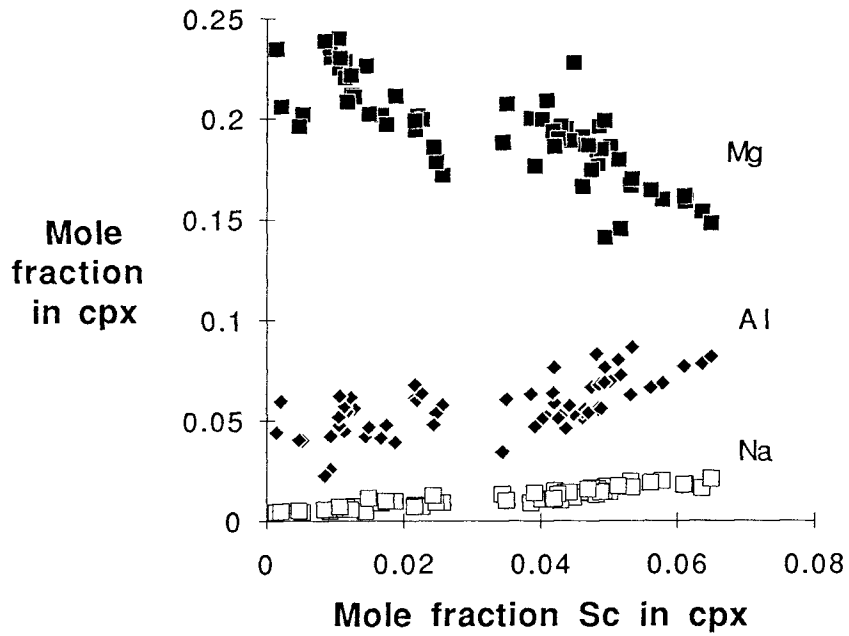


Figure 9 Covariation of major elements with Sc in clinopyroxenes.



INTERPRETATION OF RESULTS

REE and Y Partitioning

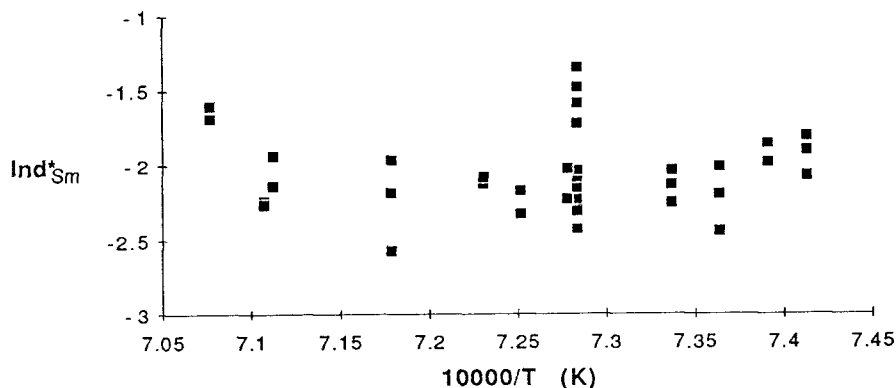
The goal of this study is to define expressions which quantify the effects of composition and temperature on the partitioning behavior of the selected trivalent cations. By defining the compositional effects, the observed scatter in D 's at individual temperatures can be compensated for and reduced, thus allowing for more precise linear regressions as functions of temperature.

An initial attempt to compensate for the compositional effects on partitioning is made by calculating compensated partition coefficients, d^* (after Lemarchande et al., 1987). Using a variation (Nielsen, 1988) of the two-lattice melt model of Bottinga and Weill (1972) to calculate melt component activities, d^* is defined as;

$$d^* = X_i^{xtl} / a_i^{liq} \quad 9$$

where X_i^{xtl} is the mole fraction of component i in the clinopyroxene and a_i^{liq} is the activity of component i in the melt. The effect of this application is shown in a plot of the logarithm of d^*_{Sm} (Fig. 10) and can be compared with the logarithm of D_{Sm} (Fig. 5b) at different temperatures. Selecting the data from figures 5b and 10 with the largest variation (1090-1110°C), a minor increase in the precision of predicted partitioning behavior, 37 to 35% (1σ) is accomplished by using d^* . This minor increase in precision is not adequate to reduce the error included in a linear regression. Thus, another approach is required to reduce the compositional effects on calculated partitioning behavior.

Figure 10 Compensated partition coefficients for Sm, calculated by applying two-lattice melt component activity model.



Ideally, any method for describing compositional effects on trace element partitioning will incorporate complete mineral component reactions. However, several obstacles have prevented this approach in previous investigations of REE. In particular, insufficient experimental data existed to adequately define the partitioning behavior of REE in terms of a clinopyroxene component reaction. Specifically, the nature of the charge balancing mechanism for the incorporation of a trivalent REE in a divalent crystal site remained unclear (Ray et al., 1983; Colson et al., 1989). In addition, the propagation of analytical error in full equilibrium reactions had not resulted in greater precision than that associated with D 's.

Using results from the factor analysis on the experimental data base, an attempt is made to define mineral-melt equilibria reactions for complete REE clinopyroxene components whose equilibrium constants demonstrate greater precision than D 's or d^* 's.

A first consideration in a REE clinopyroxene component is the charge-balancing coupled substitution. The increased D_{REE} with increasing Al in the melt (Fig. 6a) tends to confirm the coupled substitution of REE and Al in clinopyroxene proposed by Colson et al. (1989). By increasing the activity of Al in the melt and assuming a coupled substitution, the concentration of a Sm-Al clinopyroxene component would increase. Implicit in this substitution is the clinopyroxene site locations for Sm (M) and Al (T).

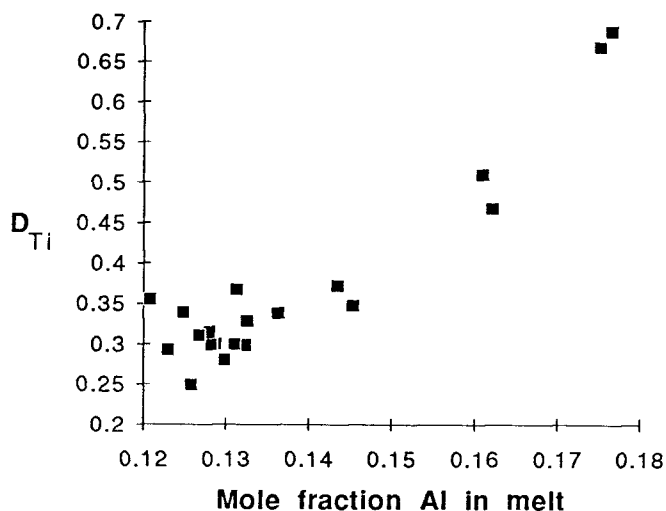
The correlation of D_{REE} with clinopyroxene Wo (Fig. 6b) confirms the findings of McKay et al. (1986). This suggests that the same conditions that enhance increased Wo contents also increase REE distribution coefficients. As the clinopyroxene structure becomes more "open" to the large Ca cation, it should also be more compatible to the large REE cations.

Assuming that Sm and Al occupy an M and a T site, respectively, the next consideration in a full clinopyroxene component is the occupancies of the other M and T sites. The correlation of D_{REE} with clinopyroxene Ti content (Fig. 6c) could be interpreted as evidence for a REE-Ti-Al clinopyroxene component. With this assumption, the stoichiometry of the component can be defined two ways, (1) $\text{SmTi}_{0.5}\text{AlSiO}_6$, and (2) SmFMTiAlO_6 where FM is any divalent ferromagnesian ion with a radius appropriate for the M sites. However, each component contains elemental site occupancies that are considered unlikely. In the first component, the charge balancing mechanism results in a large fraction of site vacancies. For every two mole fractions of REE substituting into the pyroxene there is one mole fraction of M1 sites left vacant. The charge balancing mechanism in the second component does not

result in lattice vacancies. However, a search of published spectroscopic studies on pyroxenes (e.g. Goldman and Rossman, 1979) finds no reference to what, if any, conditions Ti^{4+} occurs in T sites. In addition, the activity of either of the defined REE-Ti components would be expected to increase with increasing Ti content of the melt. This is not evident in figure 7a.

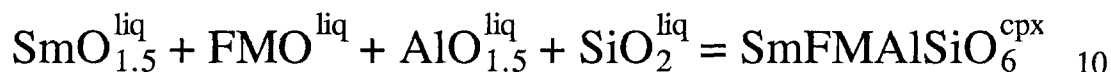
Another explanation for the correlation is that REE and Ti may be partitioning between clinopyroxene and glass in a similar fashion. This is supported by the relationship between the two distribution coefficients (Fig. 6d). With this evidence, the Al content in the melt is expected to affect D_{Ti} similarly to D_{REE} . Figure 11 indicates a positive correlation between the mole fraction of Al in the melt and D_{Ti} . Based on this result, it is concluded that the correlation of REE and Ti partitioning behavior is a consequence of both being related to a common factor and not a REE-Ti component.

Figure 11 Correlation of D_{Ti} with Al content of the melt.



The lack of correlation between D_{REE} and Fe/Mg ratios of the clinopyroxene (Fig. 7b) or melt (Fig. 7c) would suggest that the formation of an REE component is independent of the divalent ferromagnesian element on the M sites. Thus, a simplifying assumption can be made that the ratio of the activity of the ferromagnesian (FM) in the M sites to its activity in the melt is constant at any single temperature.

With the assumption of a constant D_{FM} , and assuming that Si occupies the other T site, the mineral-melt reaction for a full Sm clinopyroxene component can be expressed as:



The equilibrium constant, K , for equation 10 is defined as:

$$K = \left(\frac{a_{\text{Sm}}^{\text{cpx}}}{(a_{\text{SmO}_{1.5}}^{\text{liq}})(a_{\text{AlO}_{1.5}}^{\text{liq}})(a_{\text{SiO}_2}^{\text{liq}})} \right) \left(\frac{a_{\text{FM}}^{\text{cpx}}}{a_{\text{FMO}}^{\text{liq}}} \right) \quad 11$$

Rewriting equation 11, assuming a constant D_{FM} at any temperature, produces equation 12:

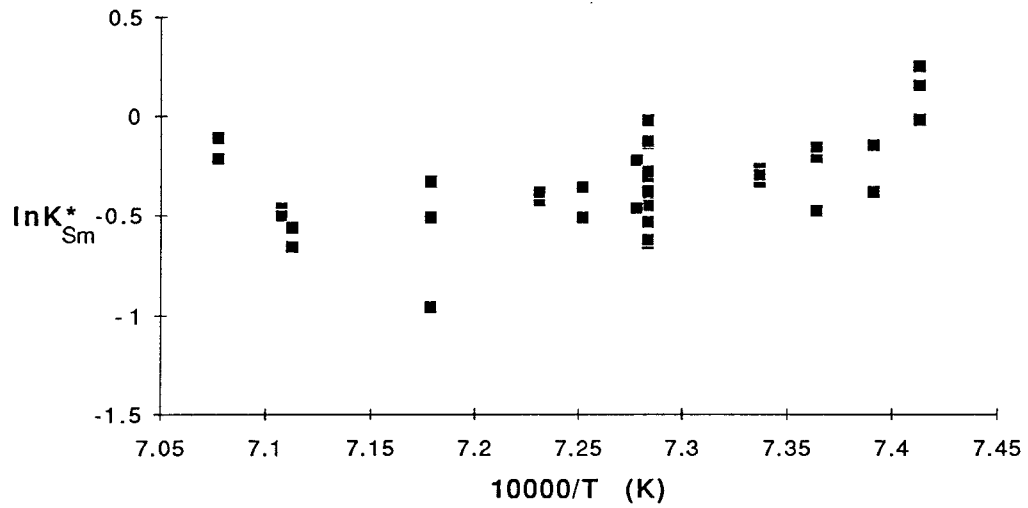
$$K^* = K * \left(\frac{a_{\text{FMO}}^{\text{liq}}}{a_{\text{FM}}^{\text{cpx}}} \right) = \left(\frac{a_{\text{Sm}}^{\text{cpx}}}{(a_{\text{SmO}_{1.5}}^{\text{liq}})(a_{\text{AlO}_{1.5}}^{\text{liq}})(a_{\text{SiO}_2}^{\text{liq}})} \right) \quad 12$$

where K^* incorporates D_{FM} and thus, is still assumed constant at any T. Using the defined equilibrium constant, the Sm content of equilibrium clinopyroxenes can now be calculated at a single temperature.

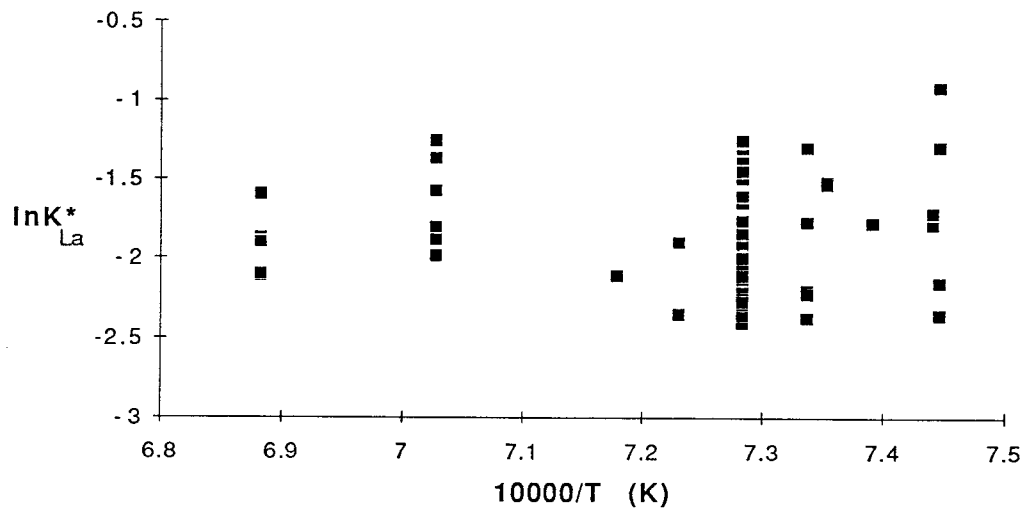
As with the calculated D's and d^* 's for Sm, the equilibrium constants for a full Sm clinopyroxene component indicate a dependence on inverse temperature (Fig. 12a). However, the scatter in calculated partitioning behavior at any temperature is significantly reduced. By choosing the data with largest scatter (1090-1110°C), the calculated K^* 's indicate a precision of 16% (1σ), which is greater than 50% increase in precision over the use of D's or d^* 's. Thus, the use of K^* 's allows for increased precision in a linear regression over the experimental temperature range. Calculated equilibrium constants for the other REE and Y over the experimental temperature range are shown in figures 12b-f.

Figure 12 Plot of the logarithm of calculated equilibrium constants for mineral-melt equilibria reactions of clinopyroxene components for (a) Sm, (b) La, (c) Gd, (d) Ho, (e) Lu, and (f) Y.

(a)



(b)



(c)

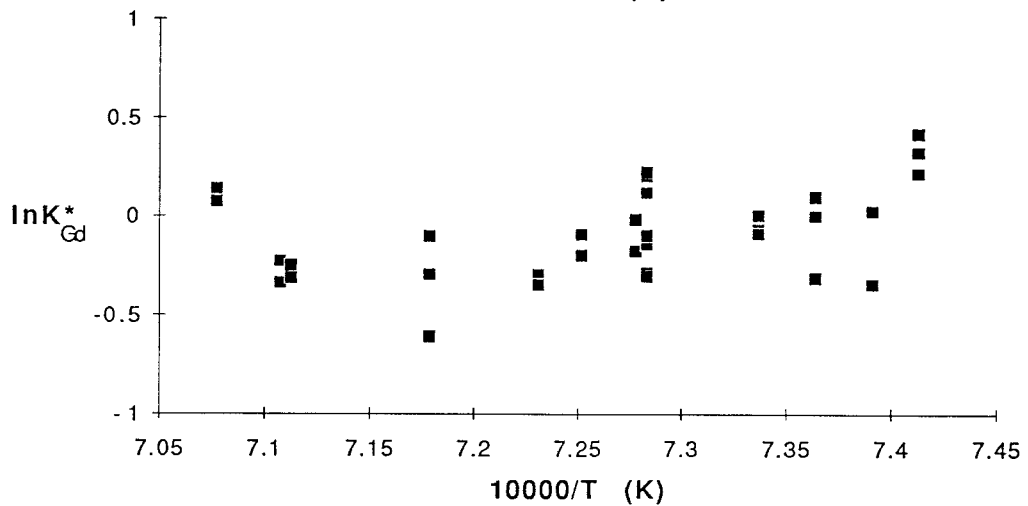
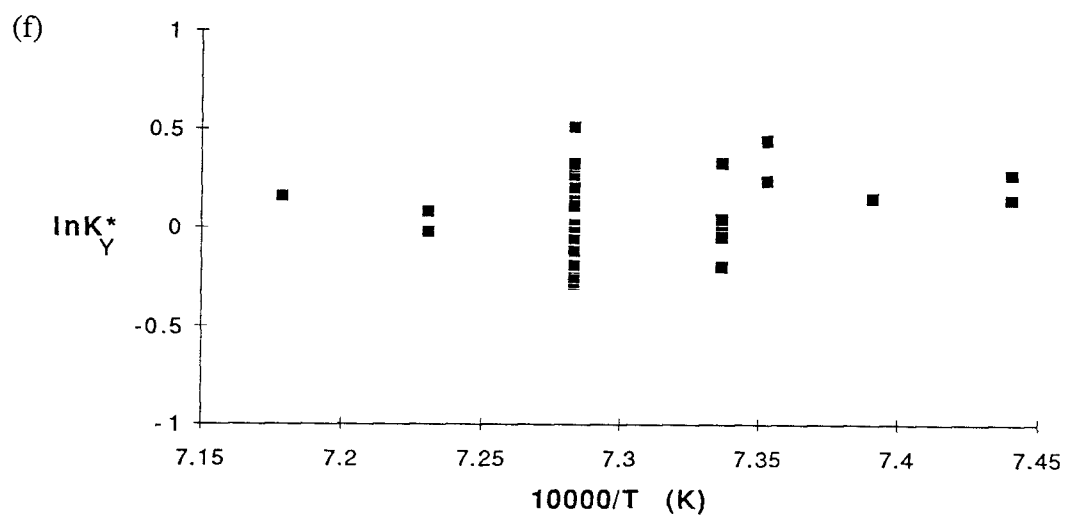
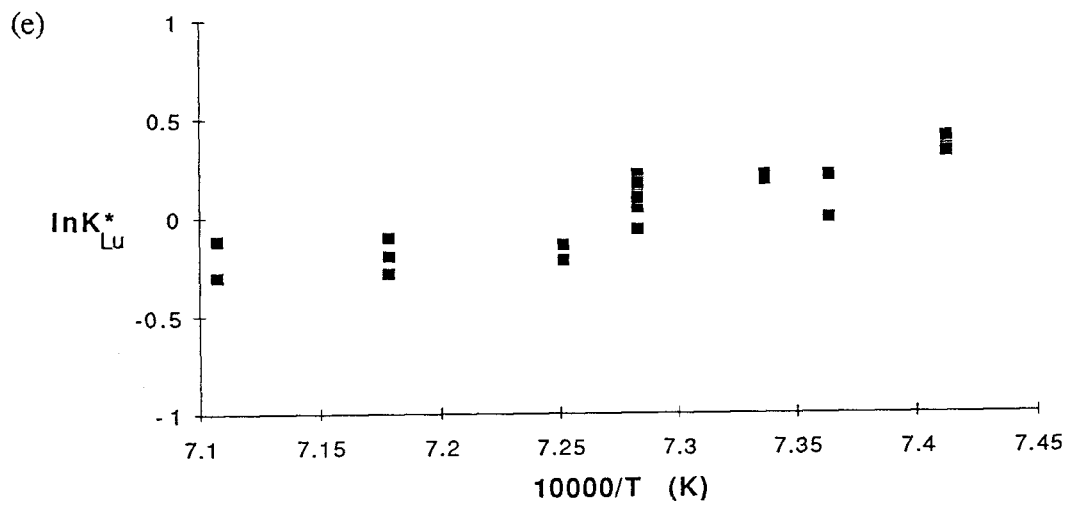
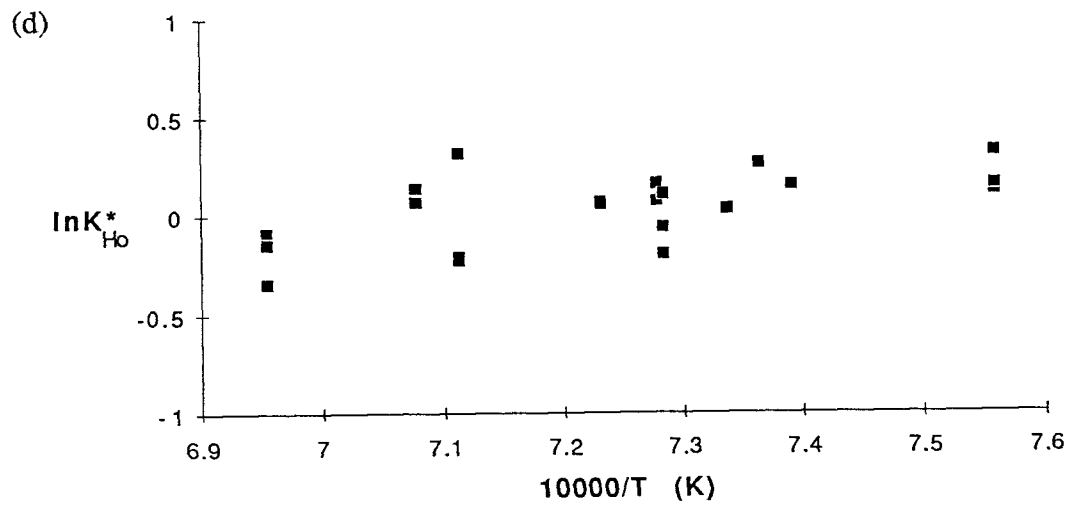


Figure 12 Continued



Linear regression of the calculated K^* 's from the experimental data set yields the following temperature functions, with 1σ precisions in parentheses:

$$\ln K_{La}^* = 119(2847) / T (^{\circ}\text{K}) - 1.95(0.29) \quad (19.8\%) \quad 13$$

$$\ln K_{Sm}^* = 11371(3521) / T (^{\circ}\text{K}) - 8.60(0.35) \quad (14.3\%) \quad 14$$

$$\ln K_{Cd}^* = 8959(3465) / T (^{\circ}\text{K}) - 6.62(0.35) \quad (13.0\%) \quad 15$$

$$\ln K_{Ho}^* = 5110(1897) / T (^{\circ}\text{K}) - 3.65(0.19) \quad (10.1\%) \quad 16$$

$$\ln K_{Lu}^* = 19704(2704) / T (^{\circ}\text{K}) - 14.29(0.27) \quad (7.3\%) \quad 17$$

$$\ln K_Y^* = 12084(6298) / T (^{\circ}\text{K}) - 8.81(0.63) \quad (9.4\%) \quad 18$$

The demonstrated effects of Wo on partitioning behavior (Fig. 6b) confirms the findings of McKay et al. (1986). This dependence is investigated by including Wo as an independent variable, along with temperature, in multiple regressions on K^* . The regressions, including precisions, are listed below:

$$\ln K_{La}^* = 162/T(^{\circ}\text{K}) - 0.58*Wo - 1.80 \quad (19.7\%) \quad 19$$

$$\ln K_{Sm}^* = 19672/T(^{\circ}\text{K}) + 2.79*Wo - 15.48 \quad (11.9\%) \quad 20$$

$$\ln K_{Cd}^* = 16500/T(^{\circ}\text{K}) + 2.54*Wo - 12.86 \quad (12.4\%) \quad 21$$

$$\ln K_{Ho}^* = 6009/T(^{\circ}\text{K}) + 0.59*Wo - 4.49 \quad (10.7\%) \quad 22$$

$$\ln K_{Lu}^* = 25597/T(^{\circ}\text{K}) + 1.79*Wo - 19.12 \quad (12.7\%) \quad 23$$

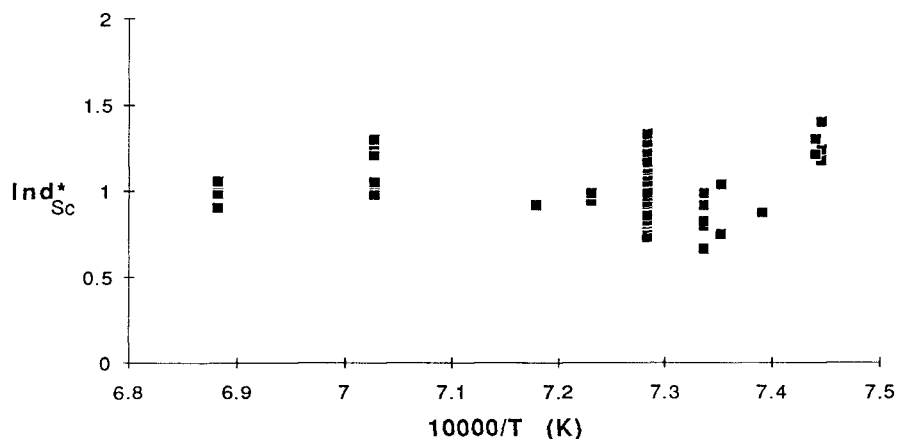
$$\ln K_Y^* = 12453/T(^{\circ}\text{K}) + 2.01*Wo - 9.73 \quad (9.6\%) \quad 24$$

The precision of the multiple regressions on K^* (Eq. 19-24) indicate no significant increase when compared to the linear regressions (Eq. 13-18). A possible explanation for this is the interdependence of Ca partitioning in clinopyroxene and the temperature of the system. This interdependence is evident in the regression constants of equations 19-24, where the trend of the W_o constants mirrors that of the enthalpy constants. Consequently, multiple regressions using temperature, and another variable which is itself a function of temperature, fail to significantly increase the precision of the linear regressions on K^* .

Sc Partitioning

Defining the compositional effects on Sc partitioning in clinopyroxene can be approached in a similar manner as REE partitioning. An initial attempt to compensate for the large scatter in D_{Sc} at individual temperatures is to calculate d_{Sc}^* . The effect of this application is seen in a comparison between the logarithm of d_{Sc}^* (Fig. 13) and the logarithm of D_{Sc} (Fig. 8) at different temperatures. Selecting data from figures 8 and 13 with the largest variation (1090-1110°C), a minor increase in the precision of predicted partitioning behavior, 20 to 17% (1σ), is accomplished by using d^* . An attempt to increase the precision of calculated partitioning behavior is made by using the experimental results to define a mineral-melt equilibria reaction for a complete Sc clinopyroxene component.

Figure 13 Compensated partition coefficients for Sc, calculated by applying two-lattice melt component activity model.



The covariation of Al, Na, and Mg with the Sc content of the clinopyroxenes (Fig. 9) suggests that Sc is paired with Al, and to a lesser extent Na. These NaSc and ScAl components substitute primarily for Mg on the M1 crystallographic site. This result is consistent with the substitution mechanisms proposed by Lindstrom (1976) and Colson et al. (1989).

Given the assumption that Sc is paired with Al in a clinopyroxene component, a one-to-one correlation is expected in the clinopyroxene Sc content and the Al content of the tetrahedral site. A test of this proposed substitution mechanism can be made by calculating the tetrahedral Al "allocated" for Sc in the pyroxene. This is accomplished by subtracting the contribution of other components from the Al content of the tetrahedral site as follows:

$$X_{Al_{Sc}}^T = [(0.5 - X_{Si}^{cpx}) - (2 * X_{Ti}^{cpx}) - (X_{Al}^{cpx} - X_{Al}^T)] \quad 25$$

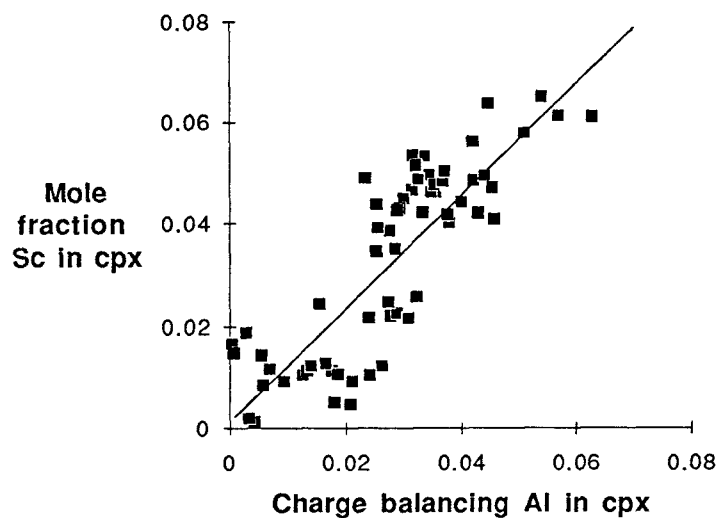
where $X_{Al_{Sc}}^T$ is the mole fraction of Al on a T site not required to charge balance other clinopyroxene components; $(0.5 - X_{Si}^{cpx})$ defines the total Al in tetrahedral coordination, where 0.5 is the mole fraction of T sites in the crystal and X_{Si}^{cpx} is the mole fraction of Si in the crystal (all assumed tetrahedrally coordinated); $(2 * X_{Ti}^{cpx})$ is the contribution of the Ti_{T_3} component ($CaTiAl_2O_6$) to tetrahedrally coordinated Al; and, $(X_{Al}^{cpx} - X_{Al}^T)$ is the contribution of the Ca_{T_3} component ($CaAl_2SiO_6$) to tetrahedrally coordinated Al.

Equation 25 can be applied to the compositions of the experimental clinopyroxenes to calculate the tetrahedral Al available for charge balancing Sc. A comparison of the calculated charge balancing Al and the Sc content of the clinopyroxene is shown in figure 14. Linear regression of the data provides the following relationship:

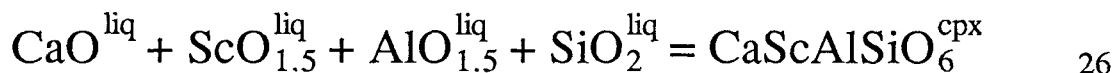
$$X_{Sc}^{cpx} = 1.09(X_{Al_{Sc}}^T) + 0.003 \quad 26$$

The differences between 1.09 and 1.0 in the slope, and 0.003 and 0.0 in the intercept, indicate that the amount of Sc attributable to a Na-Sc clinopyroxene component ($NaScSi_2O_6$) is insignificant.

Figure 14 Relationship of Sc content in the clinopyroxene with the tetrahedral Al, as calculated by equation 25, available to charge balance a CaScAlSiO_6 component. Plot of linear regression, equation 26, is shown.



Based on the results of the factor analysis, equation 26, and following the suggestion of Lindstrom (1976) and Colson et al. (1989), a Sc clinopyroxene component is defined as:

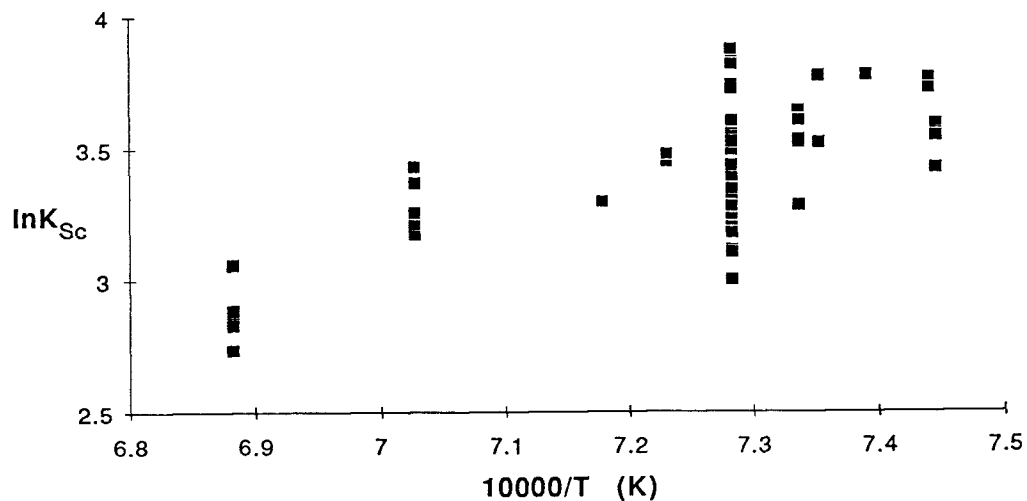


The equilibrium constant, K , for equation 26 is defined as:

$$K = \frac{a_{\text{Sc}}^{\text{cpx}}}{(a_{\text{CaO}}^{\text{liq}})(a_{\text{ScO}_{1.5}}^{\text{liq}})(a_{\text{AlO}_{1.5}}^{\text{liq}})(a_{\text{SiO}_2}^{\text{liq}})} \quad 27$$

Using the defined equilibrium constant, the Sc content of equilibrium clinopyroxenes can be calculated at a single temperature. The calculated K 's for the experimental data set indicate a dependence on inverse temperature (Fig. 15). However, the application of K 's to the data with the largest scatter (1090-1110°C) does not reduce the variability in partitioning behavior, with a precision of 23% (1σ), compared to D or d^* .

Figure 15 Plot of the logarithm of calculated equilibrium constants for mineral-melt equilibria of Sc clinopyroxene component.



Linear regression of the calculated K_{Sc} 's from the experimental data set yields the following temperature functions, with 1σ precisions in parentheses:

$$\ln K_{Sc} = 11956(1683) / T (^{\circ}\text{K}) - 5.23(0.17) \quad (12.8\%) \quad 28$$

Equation 28 indicates that the precision in K 's is improved when applied over a larger temperature range than 1090-1110°C.

TEST OF MODEL

Any empirical model must pass two tests, (1) a test of internal consistency, and (2) a test of external application. The internal consistency of the model can be determined by how well it reproduces the data set. In this case, the linear regressions of the equilibrium constants (Eq. 13-18 & 28) are applied to the experimental glass compositions in attempts to calculate the trace element contents of the coexisting clinopyroxenes. The results of these applications are shown in figures 16a-g.

Figure 16 Test results on internal precision of defined linear regressions (equations 13-18, 28) for (a) La, (b) Sm, (c) Gd, (d) Ho, (e) Lu, (f) Y, and (g) Sc.

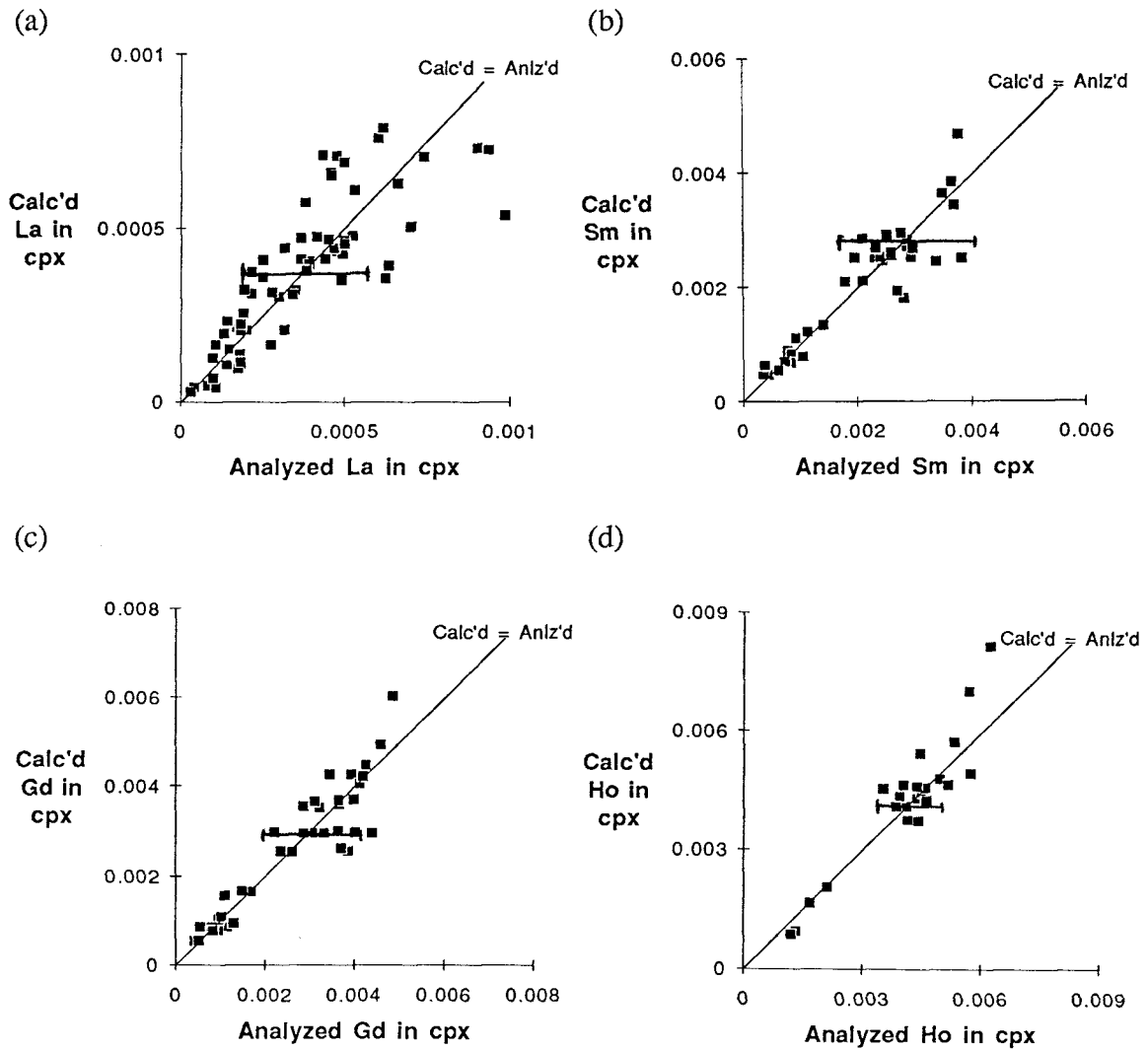
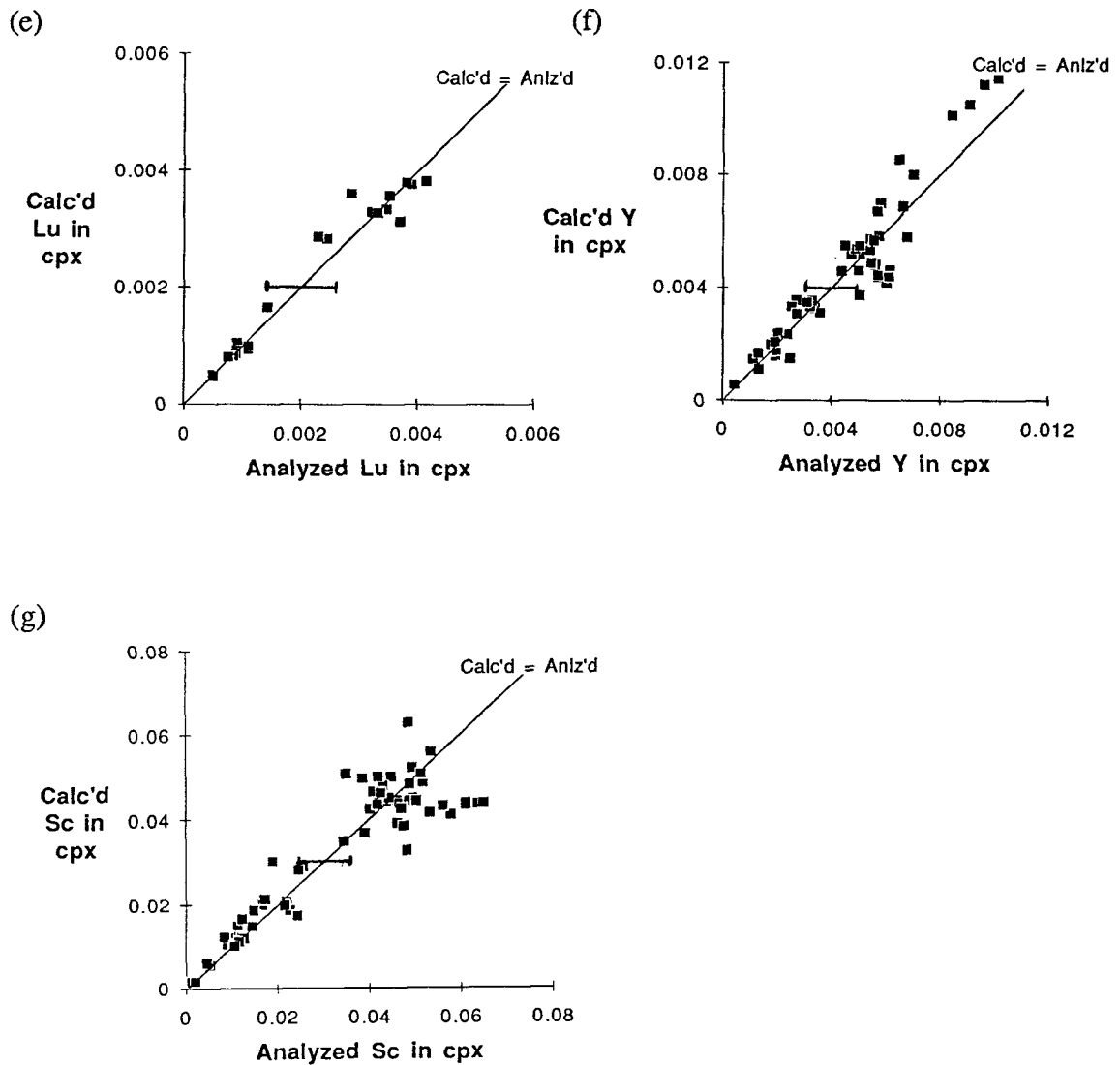


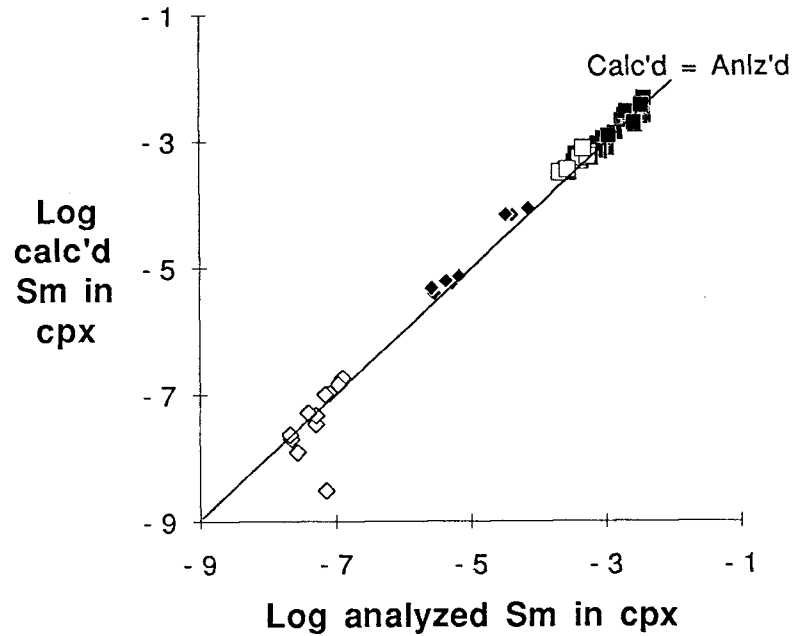
Figure 16 Continued



The external application of the calculated regressions is, in this case, limited by the lack of published 1 atmosphere experimental data on the partitioning of REE, Y, and Sc in clinopyroxene. Sufficient data exist only on Sm and Sc to evaluate the precision of the regressions at predicting partitioning behavior at higher temperatures. The single 1 atm natural system data point on Lu partitioning (McKay et al. 1986) was used to evaluate the precision of equation 17 in the temperature range of the model. Results of these external applications are shown in figures 17a-c.

Figure 17 Results of applying linear regressions of previous experimental results on (a) Sm: filled squares from current study, opens squares from McKay et al. (1986), filled diamonds from Mysen and Virgo (1980), and open diamonds from Ray et al. (1983); (b) Lu: filled squares from current study, open squares from McKay et al. (1986); and (c) Sc: filled squares from current study, open squares from Lindstrom (1976), filled diamonds from Ray et al. (1983).

(a)



(b)

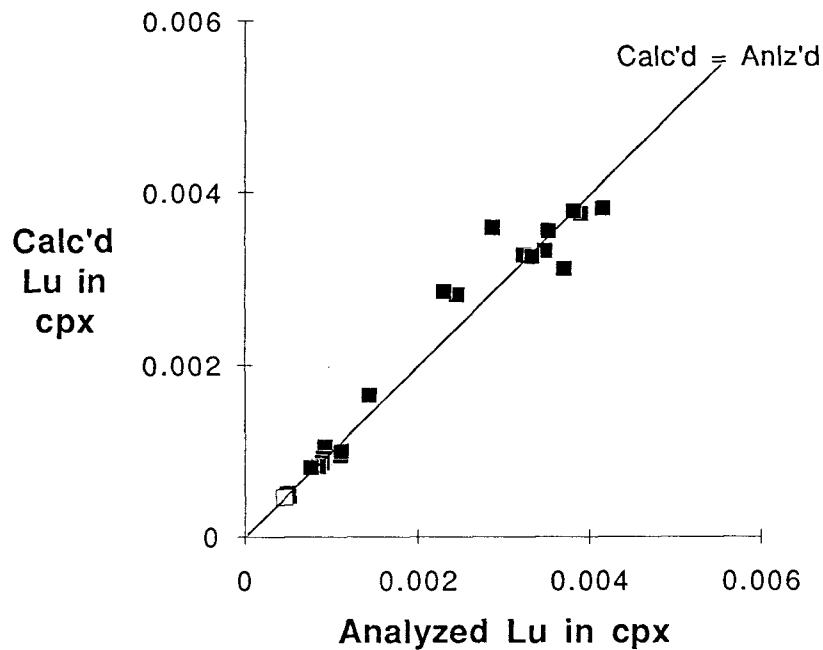
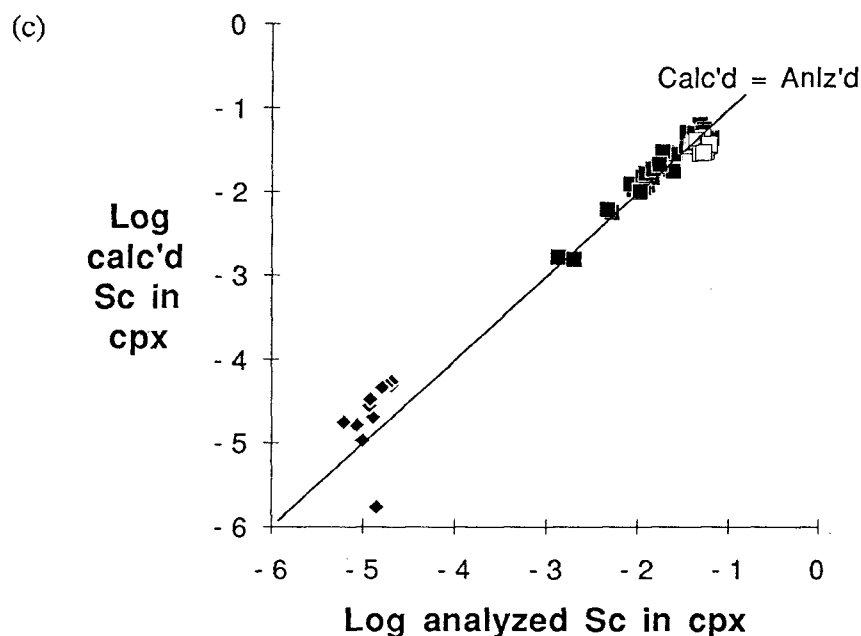


Figure 17 Continued



The regression for Sm (Eq. 14) reproduces the experimental results with a precision of 27.5% (1σ) over the temperature range of 1080-1345°C (Fig. 17a). The largest deviation occurs in the high temperature data (1300-1345°C) of Ray et al. (1983). Several characteristics may be contributing to the large deviation, 44.9% (1σ), associated with this data set. Included among these possible explanations are: (1) The temperatures are 100-150°C above the range normally associated with natural shallow mafic systems, for which the regression is calibrated; (2) The synthetic composition (Di-Ab-An) lacks components which may cause complex melt interactions, i.e. Ti and P; (3) Several melt compositions were marginally peralkaline, the two-lattice melt model does not allow for Al activities to be accurately calculated in peralkaline systems. By deleting this high temperature, synthetic system data, the reproducibility is improved to 21.6%.

The regression for Lu (Eq. 17) reproduces the single datum of McKay et al. (1986) with <1% error (Fig. 7b). The regression for Sc (Eq. 28) reproduces the experimental results with a precision of 58.0% (1σ) (Fig. 7c). Again, the largest deviation, 97.2% (1σ), occurs in the high temperature data of Ray et al. (1983). By deleting the data set, the reproducibility is improved to 20.8% (1σ). The data set of Lindstrom (1976) is reproduced with a precision of 18.4% (1σ).

Results from the tests to external data suggest that the precision of the Sm and Sc expressions may be limited to the temperatures and compositions associated with natural mafic to intermediate systems.

APPLICATION OF REGRESSIONS

The potential significance of the regressions presented above to models of igneous differentiation can be evaluated by their inclusion in an existing model for the simulation of low-pressure, mineral-melt equilibria. The model, CHAOS (Nielsen, 1989), is a modified version of an earlier program, TRACE (Nielsen, 1988). The model calculates phase compositions, proportions, and equilibrium temperatures for mafic-to-intermediate composition magmas. Crystallizing phases may be removed, or maintained in equilibrium, simulating either fractional or equilibrium crystallization. In addition, parameters to simulate magma recharge, eruption, and assimilation allow a range of open system processes to be simulated.

The mixing parameters of CHAOS are quantified in terms relative to crystallization, therefore they can be expressed as proportions of recharge, assimilation, and eruption relative to the crystallization rate. For example, a 3-0-2 model calculates the LLD for a system where for every increment of crystallization, three increments of the parent magma are recharged into the system, nothing is assimilated, and two increments are erupted from the system. This set of mixing parameters represents a system which is of constant size, i.e. recharge + assimilation = eruption + fractionation. New mineral-melt equilibria are calculated after each increment of crystallization. This approach provides a sensitive method for utilizing expressions that describe the effects of temperature and composition on phase equilibria and trace element partitioning behavior. Expressions derived by Allegre and Minster (1978) and O'Hara and Mathews (1981) attempted to quantify the effects of differentiation processes on trace element abundances. However, they assumed constant D's and phase proportions thereby limiting the range of compositions and temperatures which could be accurately modeled.

To compare the effects of the current regressions with previous methods for calculating REE LLD, a model of pure homogeneous fractional crystallization within a closed system, i.e. 0-0-0 model, was selected to simulate a static, differentiating magma chamber. A Kilauea Iki lava lake glass (olivine tholeiite), from Helz (1987), was selected as a starting composition. The sequence of crystallization for the composition was olivine, followed by augite, plagioclase, and oxides. In the sections below, the differences in the calculated LLD are examined.

The simulation calculated the LLD for the system from 0-75% crystallization. Using MgO as a measure of differentiation, the system evolved in the following

manner; 10-7.5% MgO, (0-8%) crystallization of olivine alone; 7.5-6.8% MgO, (8-16%) crystallization of augite; 6.8-6.4% MgO, (16-28%) crystallization of augite and plagioclase in the proportions 50:50; 6.4-4.8% MgO, (28-54%) crystallization of olivine, augite, and plagioclase in the proportions 10:40:50; 4.8-4.2% MgO, (54-62%) crystallization of orthopyroxene, augite, and plagioclase in the proportions 25:25:50; 4.2-3.0% MgO, (62-75%) crystallization of augite, plagioclase, and oxides in the proportions 43:43:14.

The REE ratios (La/Sm and La/Lu) are assumed to be relatively unaffected by fractional crystallization because the partition coefficients of those elements in common liquidus phases are small and similar to one another. Consequently, they are commonly used as indicators of the mantle source type (e. g. enriched or depleted) and magnitude of mantle processes (e. g. degree partial melting). From the results of the simulation (Fig. 18a & b), large variations in La/Sm using d^* (21.9% change) and D (24.6% change), and in La/Lu (16.7% change using d^* and 44.7% change using D) can be seen in the calculated LLD. However, for the simulation using K^* , the change in ratios is much smaller, 8.6% change for La/Sm and 15.5% change for La/Lu. Consequently, these results suggest that the effect of crystal fractionation on REE ratios is even smaller than previously presumed. However, because of the dependence of K^* on the Al content of the melt, crystal fractionation in systems with high Al could have a significantly larger effect.

Figure 18 Calculated REE ratios for homogeneous fractional crystallization from 0-75% for Kilauea Iki olivine tholeiite. (a) La/Sm ratios and (b) La/Lu ratios calculated using bulk D 's, d^* regressions from Nielsen (1988), and K^* regressions from current study.

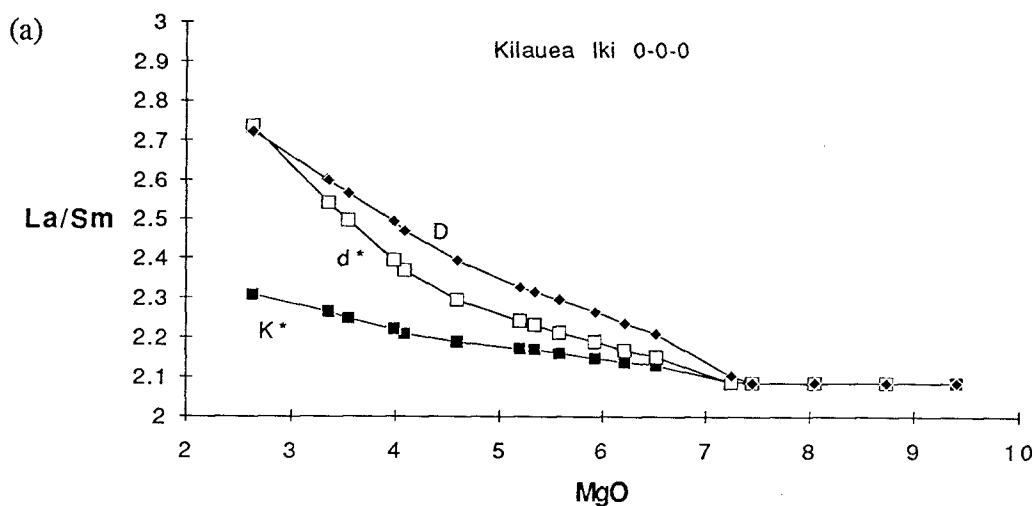
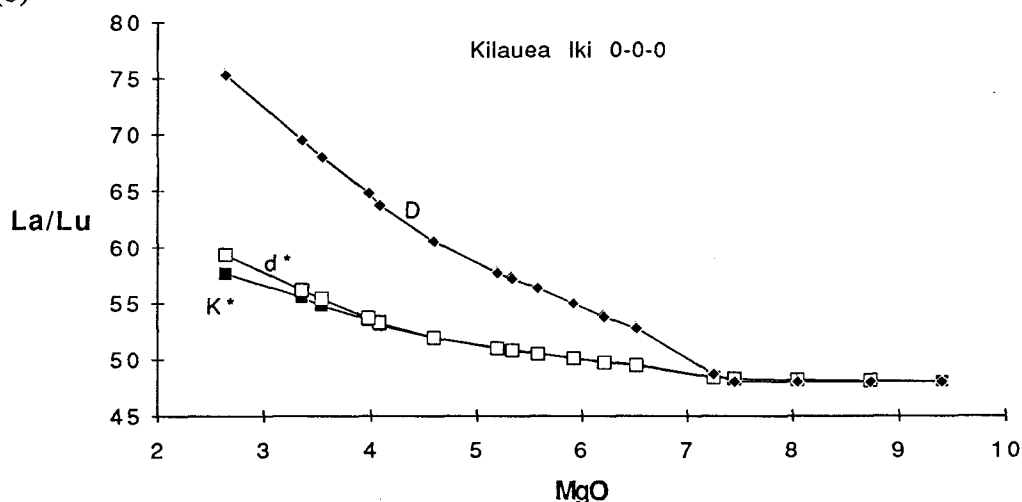


Figure 18 Continued

(b)

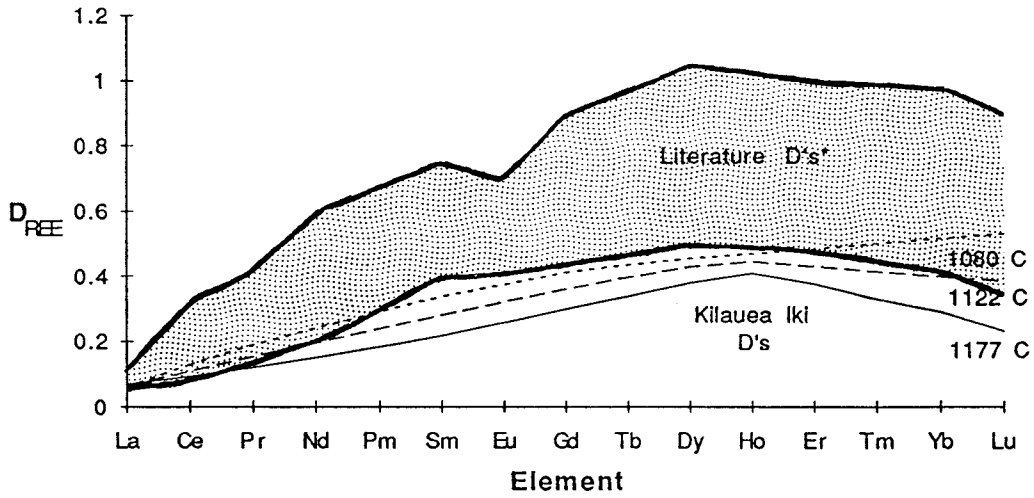


Another method of assessing the potential significance of the regressions defined in this study is by comparing distribution coefficients determined from equilibrium mineral-melt abundances calculated using the linear regressions. Using the data from the previous 0-0-0 simulation, distribution coefficients were calculated at three different temperatures. These D 's can be compared with distribution coefficients from the literature (Fig. 19). Several characteristics can be noted from figure 19. (1) The calculated D 's for this composition are significantly less than the literature values. These differences can be attributed to the "buffering effects" of Al and Si activities on REE partitioning behavior, which are included in K^* 's but not D 's. (2) The small temperature dependence of La partitioning is subordinate to the melt composition effect as the system evolves. As a result, the D for La is slightly smaller at 1080°C (0.064) than at 1177°C (0.072). (3) The relatively large temperature dependence of Lu partitioning effects the shape of the partitioning curve at lower temperatures. Figure 19 suggests that at lower temperatures (<1090°C) the HREE are more compatible than Ho.

The relatively low D 's calculated for the olivine tholeiite is likely a consequence of the low Al content of the system. Thus, the low values for D 's compared with the D 's from predominantly higher Al, calc-alkaline mafic systems is of little significance. However, the ability to predict a D for a specific temperature and composition, as demonstrated for the olivine tholeiite, is an improvement over the large range of natural D 's available from the literature. For example, the phenocryst/matrix D 's for Ho are approximately 0.75 ($\pm 50\%$) for the calc-alkaline mafic systems shown in figure 19.

Based on the results shown in figures 18 and 19, it may be inferred that potentially large errors in petrogenetic models occur by the use of fixed D's.

Figure 19 Comparison of calculated clinopyroxene REE distribution coefficients in olivine tholeiite at three different temperatures with distribution coefficients determined from phenocryst/matrix analyses from calc-alkaline mafic systems. *Data sources of literature D's: Onuma et al. (1968), Schnetzler and Philpotts (1968, 1970).



CONCLUSIONS

A method which describes REE, Y, and Sc clinopyroxene partitioning in natural mafic-to-intermediate systems as functions of temperature and melt composition has been developed. By using equilibrium constants, K^* 's, for the formation of full clinopyroxene components, the compositional effects on partitioning is reduced relative to corresponding mineral/melt D 's. The reduced scatter allows for the regression of K^* 's over a range of temperatures characteristic of natural systems to define the temperature dependence. By using the defined functions, partitioning behavior within the experimental data set can be reproduced with precisions of 7-20% (1σ). When the defined functions are applied outside of the temperature and compositional ranges on which they are calibrated, there are demonstrated limitations in their ability to accurately predict partitioning behavior in synthetic and/or peralkaline systems and at temperatures greater than those normally associated with natural magma systems.

The variability in partitioning behavior of REE and Y at any temperature appears to be dominated by melt composition effects (Al content), with relatively little crystal chemistry effects. No correlation between D_{REE} and Fe/Mg ratios is found, suggesting that the activities of REE clinopyroxene components are independent of the activities of the divalent ferromagnesian elements. In addition, the dependence of D_{REE} on W_o is interdependent with the effects of temperature on D_{REE} .

A positive correlation between D_{REE} and Ti content of the pyroxene is attributed to the effects of melt Al content on the partitioning of both REE and Ti. Because of problems with stoichiometry, the possibility of a REE-Ti-Al pyroxene component is considered unlikely.

When equilibrium constants are applied to model trace element abundances in differentiating systems, REE partitioning is dependent on the Al content of the melt. The results so far, at low pressure, suggest that partition coefficients are lower than those extrapolated from higher temperature experimental data. As a result, relatively little fractionation of REE is produced in simulations of igneous differentiation at low pressure. This contrasts with the large fractionation of REE in the same simulation using fixed D 's to model trace element abundances. As a result, potentially large additive errors may be included in petrogenetic models based on fixed distribution coefficients. What remains to be determined is the effect of pressure on the partitioning behavior of these cations.

REFERENCES

- Allegre C. J. and Minster J. F. (1978) Quantitative models of trace element behavior in magmatic processes. *Earth Planet. Sci. Lett.* **38**, 1-25.
- Allegre C. J., Treuil M., Minster J. F., Minster B., and Albarede F. (1977) Systematic use of trace elements in igneous processes: Part I: Fractional crystallization processes in volcanic suites. *Contrib. Mineral. Petrol.* **60**, 57-75.
- Bottinga Y. and Weill D. F. (1972) The viscosity of magmatic silicate liquids: A model for calculation. *Am. J. Sci.* **272**, 438-475.
- Bowen N. L. (1928) *The evolution of the igneous rocks*. Princeton Univ. Press.
- Burnham C. W. and Nekvasil H. (1986) Equilibrium properties of granite pegmatite magmas. *Am. Mineral.* **71**, 239-263.
- Casadevall T. J. and Dzurisin D. (1987) Stratigraphy and petrology of the Uwekahuna bluff section, Kilauea caldera. In Decker R. W., Wright T. L., and Stauiffer P. H., eds., *Volcanism in Hawaii*. *U.S. Geol Survey Prof. Paper* **1350**, 351-376.
- Colson R. O., McKay G. A., and Taylor L. A. (1988) Temperature and composition dependencies of trace element partitioning: Olivine/melt and low-Ca pyroxene/melt. *Geochim. Cosmochim. Acta* **52**, 539-553.
- Colson R. O., McKay G. A., and Taylor L. A. (1989) Charge balancing of trivalent trace elements in olivine and low-Ca pyroxene: A test using experimental partitioning data. *Geochim. Cosmochim. Acta* **53**, 643-648.
- Defant M. J. and Nielsen R. L. (1990) Interpretation of open system petrogenetic processes: Phase equilibria constraints on magma evolution. *Geochim. Cosmochim. Acta* **54**, 87-102.
- DePaolo D. J. (1981) Trace element and isotopic effects of combined wallrock assimilation and fractional crystallization. *Earth Planet. Sci. Lett.* **53**, 189-202.
- Dunn T. (1987) Partitioning of Hf, Lu, Ti, and Mn between olivine, clinopyroxene and basaltic liquid. *Contrib. Mineral. Petrol* **96**, 476-484.
- Drake M. J. (1972) The distribution of major and trace elements between plagioclase feldspar and magmatic silicate liquid: An experimental study. Ph.D. thesis, Univ. of Oregon, Eugene, 190 p.
- Drake M. J. (1976) Plagioclase-melt equilibria. *Geochim. Cosmochim. Acta* **40**, 457-466.
- Ellison A. J. G. and Hess P. C. (1990) Two-lattice models of trace element behavior: A response. *Geochim. Cosmochim. Acta* **54**, 2297-2302.

- Ghiorso M. S., and Carmichael I. S. E. (1985) Chemical mass transfer in magmatic processes. II. Applications in equilibrium crystallization, fractionation and assimilation. *Contrib. Mineral. Petrol.* **90**, 121-141.
- Ghiorso M. S., Carmichael I. S. E., Rivers M. L., and Sack R. O. (1983) The Gibbs Free Energy of mixing of natural silicate liquids; an expanded regular solution approximation for the calculation of magmatic intensive variables. *Contrib. Mineral. Petrol.* **84**, 107-145.
- Goldman D. S. and Rossman G. R. (1979) Determination of quantitative cation distribution in orthopyroxenes from electronic absorption spectra. *Phys. Chem. Minerals* **4**, 43-53.
- Goldschmidt V. M. (1937) The principles of distribution of chemical elements in minerals and rocks. *J. Chem. Soc. Lond.* 655-673.
- Greenland L. P. (1970) An equation for trace element distribution during magmatic crystallization. *Amer. Mineral.* **55**, 455-465.
- Helz R. T. (1987) Differentiation behavior of Kilauea Iki lava lake, Kilauea Volcano, Hawaii: An overview of past and current work. In *Magmatic Processes: Physicochemical Principles*, p 241-258.
- Henderson P. (1986) *Inorganic Geochemistry*. Pergamon.
- Hess P. C. (1977) Structure of silicate melts. *Can. Mineral.* **15**, 162-178.
- Hildreth W., Grove T. L., and Duncan M. A. (1986) Introduction to Special Section on Open Magmatic Systems. *J. Geophys. Res.* **91**, 5887-5889.
- Holland H. D. and Kulp J. L. (1949) Distribution of accessory elements in pegmatites-I. Theory: *Amer. Mineral.* **34**, 35-60.
- Huckenholz H. G., Schairer J. F., and Yoder H. S., Jr. (1969) Synthesis and stability of ferri-diopside. *Mineral. Soc. Am. Spec. Paper* **2**, 163-177.
- Irving A. J. (1978) A review of experimental studies of crystal/liquid trace element partitioning. *Geochim. Cosmochim. Acta* **42**, 743-770.
- Johnson K. T. M. (1989) Partitioning of REE, Ti, Zr, Hf, and Nb between Clinopyroxene and Basaltic liquid: an Ion Microprobe Study. *EOS Trans., Am. Geophys Union* **70**, 1388.
- Keleman P. B. and Ghiorso M. S. (1986) Assimilation of peridotite in zoned calc-alkaline plutonic complexes: Evidence from the Big Jim Complex, Washington Cascades. *Contrib. Mineral. Petrol.* **94**, 12-28.
- Kring D. A. and McKay G. A. (1984) Chemical gradients in glass adjacent to olivine in experimental charges and Apollo 15 green glass vitrophyres. *Lunar Planet. Sci.* **XV**, 461-462.
- Leeman W. P. (1974) Experimental determination of partitioning of divalent cations between olivine and basaltic liquid. Ph.D. thesis, Univ. of Oregon, Eugene, 445 p.

- Leeman W. P. and Hawkesworth C. P. (1986) Open magma systems: Trace element and isotopic constraints. *J. Geophys. Res.* **91**, 5901-5912.
- Lemarchande F., Benoit V., and Calais G. (1987) Trace element distribution coefficients in alkaline series. *Geochim. Cosmochim. Acta* **51**, 1071-1081.
- Lindstrom D. J. (1976) Experimental study of the partitioning of the transition metals between clinopyroxene and coexisting silicate liquids. Ph.D. thesis, Univ. of Oregon, Eugene, 188 p.
- McKay G. A. (1977) The petrogenesis of titanium-rich basalts from the lunar maria and of kreek-rich rocks from the lunar highlands. Ph.D. thesis, Univ. of Oregon, Eugene, 230 p.
- McKay G. A. (1986) Crystal/liquid partitioning of REE in basaltic systems: Extreme fractionation of REE in olivine. *Geochim. Cosmochim. Acta* **50**, 69-79.
- McKay G. A., Wagstaff J., and Yang S.-R. (1986) Clinopyroxene REE distribution coefficients for shergottites: The REE content of the Shergotty melt. *Geochim. Cosmochim. Acta.* **50**, 927-937.
- Michael P. J. (1988) Partition coefficients for rare earth elements in mafic minerals of high silica rhyolites: The importance of accessory mineral inclusions. *Geochim. Cosmochim. Acta* **52**, 275-282.
- Minster J. F., Minster J. B., Treuil M., and Allegre C. J. (1977) Systematic use of trace elements in igneous processes: Part II. Inverse problem of the fractional crystallization process in volcanic suites. *Contrib. Mineral. Petrol.* **61**, 49-77.
- Moore R. B., Helz R. T., Dzurisin D., Eaton G. P., Koyanagi R. Y., Lipman P. W., Lockwood J. P., and Puniwai G. S. (1980) The 1977 eruption of Kilauea volcano, Hawaii. *J. Volcan. Geotherm Res.* **7**, 189-210.
- Mysen B. O. and Virgo D. (1980) Trace element partitioning and melt structure: An experimental study at 1 atm. pressure. *Geochim. Cosmochim. Acta* **44**, 1917-1930.
- Neal C. A., Duggan T. J., Wolfe E. W., and Brandt E. L. (1988) Lava samples, temperatures, and compositions. In Wolfe E. W., ed., The Puu Oo eruption of Kilauea volcano, Hawaii: Episodes 1 through 20, January 3, 1983, through June 8, 1984. *U.S. Geol. Survey Prof. Paper* **1463**, 99-126.
- Neumann H. (1948) On hydrothermal differentiation. *Econ. Geol.* **43**, 77-83.
- Neumann H., Mead J., and Vitaliano C. J. (1954) Trace element variation during fractional crystallization as calculated from the distribution law. *Geochim. Cosmochim. Acta* **6**, 90-99.
- Nichols J., Russell J. K., and Stout M. Z. (1986) Testing magmatic hypotheses with thermodynamic modelling. In: C. M. Scarfe, ed., *Mineral. Assoc. Canada Short Course in Silicate Melts* **12**, 210-235.

- Nielsen R. L. (1985) A method for the elimination of the compositional dependence of trace element distribution coefficients. *Geochim. Cosmochim. Acta* **49**, 1775-1779.
- Nielsen R. L. (1988) A model for the simulation of combined major and trace element liquid lines of descent. *Geochim. Cosmochim. Acta* **52**, 27-38.
- Nielsen R. L. (1989) Phase equilibria constraints on AFC generated liquid lines of descent: Trace element and Sr and Nd isotopes. *J. Geophys. Res.* **94**, 787-794.
- Nielsen R. L. and Drake M. J. (1979) Pyroxene-melt equilibria. *Geochim. Cosmochim. Acta* **42**, 817-831.
- Nielsen R. L. and Dungan M. A. (1983) Low pressure mineral-melt equilibria in natural anhydrous mafic systems. *Contrib. Mineral. Petrol.* **84**, 310-326.
- Nielsen R. L. and Gallahan W. E. (1990) In defense of the two-lattice melt model: A comment on Ellison and Hess. *Geochim. Cosmochim. Acta* **54**, 2293-2295.
- O'Hara M. J. and Mathews R. E. (1981) Geochemical evolution in an advancing, periodically replenished, periodically tapped, continuously fractionated magma chamber. *J. Geol. Soc. London* **138**, 237-277.
- Onuma N., Higuchi H., Wakita H., and Nagasawa H. (1968) Trace element partition between two pyroxenes and the host lava. *Earth Planet. Sci. Lett.* **5**, 47-51.
- Porter S. C., Garcia M. O., Lockwood J. P., and Wise W. S. (1987) Guidebook for Mauna Loa-Mauna Kea-Kohala field trip. Hawaii symposium on how volcanoes work. 40 p.
- Ray G. L., Shimizu N., and Hart S. R. (1983) An ion microprobe study of the partitioning of trace elements between clinopyroxene and liquid in the system diopside-albite-anorthite. *Geochim. Cosmochim. Acta* **47**, 2131-2140.
- Rhodes J. M. (1988) Geochemistry of the 1984 Mauna Loa eruption: Implications for magma storage and supply. *J. Geophys. Res.* **93**, 4453-4466.
- Richardson F. D. (1956) Activities in ternary silicate melts. *Trans Faraday Soc.* **52**, 1312-1324.
- Shnetzler C. C. and Philpotts J. A. (1968) Partition coefficients of rare-earth elements and barium between igneous matrix material and rock-forming-mineral phenocrysts-I. In: Ahrens L. H. (ed) *Origin and distribution of the elements*. Pergamon, 929-938.
- Shnetzler C. C. and Philpotts J. A. (1970) Partition coefficients of rare-earth elements between igneous matrix material and rock-forming-mineral phenocrysts-II. *Geochim. Cosmochim. Acta* **34**, 331-340.
- Sisson T. W. (1989) Clinopyroxene-Rhyolite Trace Element Partition Coefficients Measured by Ion Microprobe. *EOS Trans., Amer. Geophys. Union* **70**, 1403.

- Toop G. W. and Samis C. S. (1962) Activities of ions in silicate melts. *Trans. Metal. Soc. A.I.M.E.* **224**, 878-887.
- Watson E. B. (1985) Henry's law behavior in simple systems and in magmas: Criteria for discerning concentration-dependent partition coefficients in nature. *Geochim. Cosmochim. Acta* **49**, 917-923.
- Williams R. J. and Mullins O. (1981) JSC systems using solid ceramic oxygen electrolyte cells to measure oxygen fugacities in gas mixing systems. *NASA TMX-58234*, 37 p.
- Wright T. L. and Fiske R. S. (1971) Origin of the differentiated and hybrid lavas of Kilauea volcano, Hawaii. *J. Petrol.* **12**, 1-65.

APPENDIX

PYROXENES (La, Y, Sc doped)

System	Charge	T (C)	Analysis Ref #	Na	Mg	Al	Si	K	Ca	Ti	Mn	Cr	Fe	Sc	Y	La
GC-68	a344	1100	1	0.0190	0.1640	0.0662	0.4318	0.0002	0.1853	0.0140	0.0018	0.0002	0.0558	0.05617	0.00506	0.00045
	a344	1100	2	0.0194	0.1666	0.0628	0.4389	0.0002	0.1842	0.0129	0.0017	0.0002	0.0545	0.05326	0.00474	0.00042
	1d	1100	1	0.0124	0.1858	0.0481	0.4519	0.0002	0.1934	0.0164	0.0018	0.0002	0.0641	0.02431	0.00135	0.00018
ML-190	a	1100	1	0.0101	0.2071	0.0607	0.4490	0.0001	0.1573	0.0064	0.0016	0.0007	0.0672	0.03499	0.00451	0.00038
	a	1100	2	0.0111	0.1859	0.0765	0.4306	0.0000	0.1744	0.0097	0.0015	0.0012	0.0610	0.04200	0.00556	0.00053
	a72	1100	1	0.0106	0.1994	0.0507	0.4484	0.0002	0.1530	0.0073	0.0022	0.0005	0.0814	0.04017	0.00571	0.00046
	a72	1100	2	0.0108	0.1937	0.0638	0.4400	0.0001	0.1564	0.0093	0.0015	0.0007	0.0749	0.04178	0.00663	0.00046
	a192	1100	1	0.0101	0.1960	0.0524	0.4504	0.0000	0.1587	0.0087	0.0017	0.0008	0.0727	0.04293	0.00488	0.00048
	a192	1100	2	0.0089	0.1999	0.0631	0.4455	0.0001	0.1606	0.0092	0.0013	0.0008	0.0667	0.03856	0.00505	0.00043
	a192	1100	3	0.0109	0.2087	0.0521	0.4428	0.0000	0.1511	0.0083	0.0022	0.0007	0.0760	0.04088	0.00581	0.00050
ML-176	1d	1100	1	0.0056	0.2385	0.0228	0.4768	0.0001	0.1597	0.0090	0.0024	0.0008	0.0744	0.00852	0.00132	0.00013
	1d	1100	1	0.0056	0.2204	0.0569	0.4565	0.0001	0.1691	0.0085	0.0017	0.0006	0.0671	0.01138	0.00198	0.00011
	1d	1100	2	0.0055	0.2218	0.0614	0.4533	0.0000	0.1623	0.0090	0.0017	0.0009	0.0696	0.01223	0.00206	0.00018
TLW67	4a	1090	1	0.0156	0.1865	0.0538	0.4383	0.0002	0.1633	0.0120	0.0014	0.0001	0.0757	0.04701	0.00544	0.00050
	4a	1090	2	0.0143	0.1886	0.0575	0.4392	0.0001	0.1543	0.0121	0.0017	0.0009	0.0810	0.04424	0.00575	0.00032
	6a	1100	1	0.0134	0.1896	0.0512	0.4488	0.0002	0.1511	0.0112	0.0016	0.0008	0.0838	0.04254	0.00544	0.00037

GLASSES (La,Y,Sc doped)

System	Charge	T (C)	Analysis Ref #	Na	Mg	Al	Si	P	K	Ca	Ti	Mn	Cr	Fe	Sc	Y	La
ML-190	a72	1100	2	0.0401	0.0728	0.1257	0.4733	0.0037	0.0088	0.0839	0.0278	0.0017	0.0000	0.1145	0.01808	0.01829	0.01111
	a192	1100	1	0.0402	0.0736	0.1257	0.4827	0.0034	0.0105	0.0849	0.0286	0.0017	0.0000	0.1049	0.01846	0.01377	0.01164
	a192	1100	2	0.0405	0.0728	0.1268	0.4853	0.0033	0.0103	0.0843	0.0284	0.0014	0.0000	0.1031	0.01862	0.01368	0.01135
	a192	1100	3	0.0390	0.0741	0.1278	0.4764	0.0045	0.0100	0.0831	0.0289	0.0023	0.0000	0.1062	0.01862	0.01782	0.01125
ML-176	1d	1100	1	0.0428	0.0879	0.1256	0.5233	0.0040	0.0096	0.0819	0.0324	0.0017	0.0000	0.0811	0.00357	0.00354	0.00265
	1d	1100	1	0.0389	0.0837	0.1227	0.4939	0.0034	0.0078	0.0930	0.0249	0.0018	0.0000	0.1179	0.00499	0.00436	0.00262
TLW67	1d	1100	2	0.0425	0.0631	0.1348	0.4990	0.0036	0.0084	0.0915	0.0264	0.0018	0.0000	0.1163	0.00465	0.00499	0.00303
	4a	1090	1	0.0418	0.0694	0.1283	0.4655	0.0042	0.0134	0.0816	0.0350	0.0018	0.0000	0.1185	0.01763	0.01483	0.00805
	4a	1090	2	0.0412	0.0679	0.1301	0.4697	0.0045	0.0129	0.0811	0.0340	0.0017	0.0000	0.1174	0.01773	0.01437	0.00746
	6a	1100	1	0.0400	0.0723	0.1338	0.4656	0.0042	0.0112	0.0855	0.0319	0.0015	0.0000	0.1149	0.01808	0.01344	0.00760

GLASSES (Sm,Gd,Ho,Lu doped)

System	Charge	T (C)	Analysis Ref #	Na	Mg	Al	Si	P	K	Ca	Ti	Mn	Cr	Fe	Sm	Gd	Ho	Lu	
H87-3	2b	1134	1	0.0504	0.0787	0.1442	0.4751	0.0055	0.0191	0.0984	0.0168	0.0013	0.0000	0.0800	0.01044	0.01057	-----	0.00950	
	2b	1134	2	0.0490	0.0792	0.1438	0.4742	0.0069	0.0180	0.0978	0.0175	0.0015	0.0000	0.0809	0.01084	0.01033	-----	0.00994	
	3b	1140	1	0.0394	0.0921	0.1589	0.4543	0.0026	0.0078	0.1214	0.0199	0.0010	0.0000	0.0815	0.00632	0.00679	0.00777	-----	
	3b	1140	2	0.0405	0.0904	0.1613	0.4564	0.0026	0.0080	0.1200	0.0192	0.0013	0.0000	0.0790	0.00656	0.00676	0.00758	-----	
	Ho1	1165	1	0.0350	0.1027	0.1555	0.4677	0.0020	0.0066	0.1247	0.0214	0.0014	0.0000	0.0734	-----	-----	0.00969	-----	
	Ho1	1165	2	0.0356	0.1013	0.1550	0.4645	0.0021	0.0063	0.1270	0.0216	0.0015	0.0000	0.0752	-----	-----	0.00985	-----	
	Ho1	1165	3	0.0350	0.1019	0.1535	0.4659	0.0027	0.0069	0.1274	0.0222	0.0012	0.0000	0.0734	-----	-----	0.01003	-----	
	Ho2	1133	1	0.0538	0.0798	0.1847	0.4764	0.0032	0.0100	0.1082	0.0202	0.0010	0.0000	0.0612	-----	-----	0.00142	-----	
	Ho2	1133	2	0.0551	0.0801	0.1828	0.4773	0.0026	0.0100	0.1080	0.0198	0.0013	0.0000	0.0616	-----	-----	0.00131	-----	
	43152	1e	1100	1	0.0571	0.0528	0.1453	0.4841	0.0034	0.0030	0.0907	0.0294	0.0025	0.0000	0.1281	0.00134	0.00119	-----	0.00097
1e		1100	2	0.0549	0.0523	0.1435	0.4860	0.0036	0.0029	0.0915	0.0300	0.0020	0.0000	0.1296	0.00137	0.00124	-----	0.00092	
Ho1		1050	1	0.0466	0.0361	0.1052	0.4911	0.0056	0.0056	0.0864	0.0300	0.0025	0.0000	0.1789	-----	-----	0.01197	-----	
Ho1		1050	2	0.0458	0.0371	0.1036	0.4869	0.0065	0.0056	0.0874	0.0301	0.0032	0.0000	0.1820	-----	-----	0.01180	-----	
Ho1		1050	3	0.0561	0.0398	0.1542	0.4924	0.0036	0.0032	0.0874	0.0283	0.0023	0.0000	0.1259	-----	-----	0.00673	-----	
1e		1100	1	0.0523	0.0666	0.1751	0.4889	0.0030	0.0091	0.0945	0.0238	0.0014	0.0000	0.0809	0.00161	0.00141	-----	0.00136	
3/83k	1e	1100	2	0.0516	0.0648	0.1766	0.4899	0.0027	0.0088	0.0957	0.0240	0.0011	0.0000	0.0804	0.00158	0.00152	-----	0.00130	
	1b	1106	1	0.0448	0.0692	0.1287	0.4875	0.0054	0.0114	0.0932	0.0316	0.0013	0.0000	0.1055	0.00740	0.00706	-----	0.00694	
KL77	1b	1106	2	0.0445	0.0697	0.1282	0.4874	0.0050	0.0115	0.0926	0.0314	0.0013	0.0000	0.1068	0.00741	0.00713	-----	0.00708	
	3b	1085	1	0.0454	0.0625	0.1208	0.4868	0.0044	0.0134	0.0858	0.0379	0.0015	0.0000	0.1158	0.00894	0.00860	-----	0.00817	
	3b	1085	2	0.0451	0.0608	0.1193	0.4842	0.0056	0.0131	0.0869	0.0384	0.0011	0.0000	0.1189	0.00939	0.00886	-----	0.00836	
	4b	1076	1	0.0422	0.0613	0.1151	0.4734	0.0065	0.0138	0.0871	0.0407	0.0020	0.0000	0.1297	0.00974	0.00953	-----	0.00889	
	4b	1076	2	0.0428	0.0594	0.1150	0.4767	0.0061	0.0138	0.0864	0.0409	0.0013	0.0000	0.1297	0.00957	0.00935	-----	0.00895	
	4b	1076	3	0.0393	0.0643	0.1111	0.4788	0.0056	0.0129	0.0912	0.0387	0.0016	0.0000	0.1283	0.00949	0.00950	-----	0.00902	
	5b	1090	1	0.0472	0.0716	0.1363	0.4773	0.0038	0.0123	0.0863	0.0319	0.0012	0.0000	0.1103	0.00760	0.00740	-----	0.00673	
	5b	1090	2	0.0426	0.0751	0.1230	0.4695	0.0055	0.0116	0.0888	0.0376	0.0017	0.0000	0.1183	0.00932	0.00893	-----	0.00797	
	1e	1100	1	0.0464	0.0636	0.1324	0.4924	0.0050	0.0121	0.0915	0.0381	0.0016	0.0000	0.1092	0.00285	0.00260	-----	0.00227	
	1e	1100	2	0.0464	0.0649	0.1311	0.4870	0.0058	0.0117	0.0911	0.0395	0.0018	0.0000	0.1126	0.00278	0.00288	-----	0.00225	
	E-1	b	1100	1	0.0486	0.0801	0.1299	0.4950	0.0023	0.0076	0.0804	0.0320	0.0012	0.0000	0.0741	0.01489	0.01535	0.01761	-----
		5b	1133	1	0.0413	0.1001	0.1585	0.5054	0.0023	0.0072	0.0977	0.0217	0.0011	0.0000	0.0329	0.01008	0.00992	0.01122	-----
5b		1133	2	0.0404	0.0925	0.1520	0.4840	0.0023	0.0071	0.1055	0.0212	0.0011	0.0000	0.0641	0.00902	0.01002	0.01025	-----	
2MH005	3e	1120	1	0.0542	0.0703	0.1503	0.4898	0.0079	0.0174	0.0903	0.0208	0.0019	0.0000	0.0858	0.00370	0.00392	-----	0.00373	
	2e	1080	1	0.0526	0.0533	0.1462	0.5233	0.0133	0.0281	0.0687	0.0316	0.0016	0.0000	0.0722	0.00285	0.00287	0.00315	-----	
GC-68	2e	1080	2	0.0527	0.0457	0.1530	0.5359	0.0092	0.0318	0.0617	0.0274	0.0015	0.0000	0.0747	0.00199	0.00228	0.00214	-----	
	b	1100	1	0.0409	0.0747	0.1268	0.4811	0.0041	0.0077	0.0906	0.0261	0.0017	0.0000	0.1143	0.01010	0.01010	0.01114	-----	
ML-190	b	1100	2	0.0413	0.0752	0.1258	0.4803	0.0042	0.0085	0.0902	0.0264	0.0019	0.0000	0.1147	0.00999	0.00997	0.01101	-----	
	1b	1101	1	0.0408	0.0715	0.1249	0.4836	0.0044	0.0086	0.0917	0.0266	0.0014	0.0000	0.1160	0.00940	0.01037	0.01003	-----	
	1b	1101	2	0.0416	0.0709	0.1280	0.4884	0.0037	0.0092	0.0896	0.0255	0.0011	0.0000	0.1121	0.00889	0.01130	0.00919	-----	
	2b	1085	1	0.0424	0.0639	0.1238	0.4820	0.0047	0.0104	0.0878	0.0320	0.0014	0.0000	0.1170	0.01144	0.01097	0.01167	-----	
	6b	1110	1	0.0420	0.0728	0.1325	0.4896	0.0029	0.0083	0.0934	0.0236	0.0015	0.0000	0.1062	0.00828	0.00947	0.00924	-----	
	6b	1110	2	0.0414	0.0733	0.1313	0.4933	0.0030	0.0082	0.0938	0.0232	0.0013	0.0000	0.1019	0.00849	0.01095	0.00949	-----	
ML-176	3b	1090	1	0.0391	0.0661	0.1209	0.4833	0.0036	0.0081	0.0900	0.0290	0.0014	0.0000	0.1195	0.01250	0.01241	0.01376	-----	
	1e	1100	1	0.0503	0.0668	0.1609	0.4937	0.0037	0.0103	0.0947	0.0269	0.0016	0.0000	0.0867	0.00156	0.00141	-----	0.00142	
TLW67	1e	1100	2	0.0502	0.0662	0.1622	0.4949	0.0035	0.0105	0.0939	0.0269	0.0015	0.0000	0.0857	0.00157	0.00153	-----	0.00132	
	3e	1120	1	0.0541	0.0764	0.1464	0.4970	0.0029	0.0104	0.0892	0.0304	0.0013	0.0000	0.0867	0.00164	0.00180	-----	0.00181	
	3e	1120	2	0.0525	0.0770	0.1473	0.4961	0.0037	0.0099	0.0892	0.0299	0.0015	0.0000	0.0871	0.00186	0.00195	-----	0.00176	